Special Conference Collection

BioResources

A peer-reviewed Online Journal Devoted to the Science and Advanced Applications of Lignocellulosic Resources

A collection of papers from the Italic4 Conference, "Science & Technology of Biomasses: Advances and Challenges," May 8-10, 2007, Rome, Italy

Issue Editor:
Claudia Crestini

BioResources is hosted at ***ncsu.edu/bioresources*** by North Carolina State University. *Open Journal Systems* software is used for automated submission and reviewing.

LACTOSE TO NATURALIZE TEXTILE DYES

Roberto Bianchini,*[a] Giorgio Catelani,[b] Elena Frino,[b] Jalal Isaad,[a] and Massimo Rolla[a]

Many natural dyes, for example carminic acid, are soluble in water. We present a simple strategy to naturalize synthetic azadyes through their linkage with lactose to induce their water solubility. The dyeing process of textile fibres then becomes possible in water without additives such as surfactants and mordants, which result in products that are difficult to eliminate. Glyco-azadyes (GADs) we are presenting here are obtained through a diether linker to bond the azadye and the sugar. Tinctorial tests were carried out with fabrics containing wool, polyester, cotton, nylon, and acetate. GADs were found to be multipurpose and capable of dyeing many fabrics efficiently under mild conditions.

Keywords: Lactose, Conjugation, Dyeing , Azadyes, Ethers

[a]*Dipartimento di Chimica Organica "Ugo Schiff", Università di Firenze, via della Lastruccia 13, 50019 Sesto Fiorentino (FI) (Italy), Fax: +39 0554573531, phone: +39 0554573450*
[b]*Dipartimento di Chimica Bioorganica e Biofarmacia, Università di Pisa, Via Bonanno, 33 - 56126, Pisa (Italy) * Corresponding author: roberto.bianchini@unifi.it*

INTRODUCTION

Dyeing chemistry started from an early time, during a period when the majority of dyes were extracted from natural compounds, i.e. from vegetable and animal sources. Currently the global production of textile dyes is estimated to be $7x10^5$ tons per year (Neamtu et al. 2002), and a significant part of this quantity is eliminated in the effluents of dyeing plants, polluting salt and fresh waters throughout the world.

Dyes are generally applied in an aqueous solution and they require auxiliary chemicals to improve the dyeing process. For instance, surfactants are used to increase solubility, mordants to enhance the fastness of the dye on the fibers, and salts to adjust the pH. Effluent from textile industries therefore can contain a broad spectrum of contaminants, such as highly hydrophobic dyes, suspended solids, chlorinated organic solvents, surfactants in huge concentrations, mordents, metals, etc. (Poon et al. 1999). Reactive dyes are another class of environmentally dangerous textile dyes; as the name suggests, these are very reactive molecules that form covalent bonds with fibers, but they also react with water, leading to inherent losses. Moreover, it's well known that the azo molecules can degrade to aromatic amines, which can further damage the environment if they are released (Neamtu et al. 2000). Selective treatment of effluent is not possible, because the type and extent of contamination varies, depending on the fabric dyed or the class of dye used. Because most pollutants present in the water have different physical and chemical properties, normally the chromophores are attacked using oxidative treatments of the contaminated waters (ozone, H_2O_2, UV), removing only the visible pollution (Rott and Minke 1999; Bianchini et al. 2002; Selcuk 2005). These treatments are efficient for the depletion of the colour, but the yields of these are variable and the final oxidation products (Mascolo et al. 2002) are often unknown; most importantly, the colorless oxidation products are possibly even more dangerous than the starting dyes (Pierce et al. 2003).

Because of the large variety of species present, a biological approach is also difficult. Therefore, increasing attention has been devoted to natural dyes, with the aim of finding environmentally friendly materials. Natural dyes extracted from plants or animals do not cover all the market requirements, and their isolation from natural sources is difficult.

Furthermore, the impact on the environment is far from negligible when high quantities of dye are required. These factors, together with the cost of these processes, have slowed the development of dyes based on natural products. In order to devise a new strategy to solve these problems, we initiated a naturalization of synthetic dyes, by means of their glycosylation (Bianchini et al. 2004). The aims of this attempt are multiple: a) use of carbohydrates, which are widely and cheaply available, such as lactose, or D-glucose and D-galactose; these compounds often are discarded in huge quantities to the environment, and the environmental impact should not be neglected; b) achievement of hydrophilicity of dyes through their glycoconjugation, so that dyeing processes with dispersed dyes could be carried out without surfactants, which can be very difficult to treat; c) attainment of easier dyeing processes, avoiding high temperatures and high pressures; d) increased affinity towards the textiles, improving efficacy, and reducing waste; e) possibility of efficient and more selective waste treatments using, for instance, live micro-organisms to attack the sugar moiety and consequently the covalently bonded chromophoric part, or the use of enzymes able to destroy dyes; and f) preparation of multipurpose dyes able to dye different fabrics (synthetic, natural, artificial).

On the other hand, also some natural dyes are endowed with saccharidic moieties. For instance, the well known carminic acid is such a dye, but the characteristic is more general, since the hydrosolubility is often a requirement of this class of dyes. Therefore, we devised a completely new approach, consisting on the preparation of glyco azadyes, we will call 'naturalized dyes'. The word naturalize refers to the use of a natural glycide, lactose, that in our process glycoconjugates the dye. As in carmicic acid or other similar natural compounds, a chromophore is transformed into a hydrosoluble species through glycoconjugation with a sugar.

EXPERIMENTAL

General Methods

The synthetic details of our approach are given in two recent papers (Bartalucci et al. 2007, Bianchini et al. 2007). Red azadye **1a** (Disperse Red 1) is commercially available (Sigma-Aldrich), yellow dye **1b** was prepared according to literature (Podsiadly 2003). Literature methods were used to prepare 6'-O-(1-methoxy-1-methylethyl)-2,3:5,6:3',4'-tri-*O*-isopropylidenelactose dimethyl acetal **2** (Barili et al. 1997).

To measure reflectance a spectrophotometer Varian Cary 4000 was used, endowed with reflectance apparatus. Fastness was measured according to ISO 105 (X-12) C06 standard pattern.

General Procedure for the Preparation of Protected GADs:

A mixture of the appropriate etherified sugar (1.0 mmol), KOH (4.0 equivalents) and 18-crown-6 ether (0.01 equivalent) in THF (10 ml) was stirred at room temperature for 1 hr, then the dye was added and the mixture left stirring under the same conditions for several hours. The mixture was then neutralized with a saturated aqueous solution of NH_4Cl and extracted with CH_2Cl_2. The organic phase was dried over Na_2SO_4, concentrated, and the resulting residue purified by flash chromatography.

RESULTS AND DISCUSSION

GADs are a new class of naturalized, multipurpose, glycoconjugated dyes, consisting of a synthetic, commercially available dye linked to a saccharide from natural and renewable sources (lactose, D-glucose, D-galactose). The linkage is made using a bifunctional linker.

The modification of the azadyes is carried out on their side chain in order to avoid changes on the chromophoric group and maintain their original colour. The choice of difunctional linkers to be used for the linkage of glycide and dye has been devised on the basis of their ease availability and the simplicity of the practical procedure, with the final aim of an industrial development of the new glycoazadyes. Figure 1 shows two complementary approaches to synthesis these GADs: Path "a" begins by attaching the linker to a protected glycide, while path "b" starts in the reverse order. The resulting structures are diethers, with the formation of two etheric bonds, one between the sugar and the bridge, and a second between the bridge and the hydroxyl group on the side chain of the azadye. Furthermore, the ethers have proven to be stable even under the stressful conditions of dyeing.

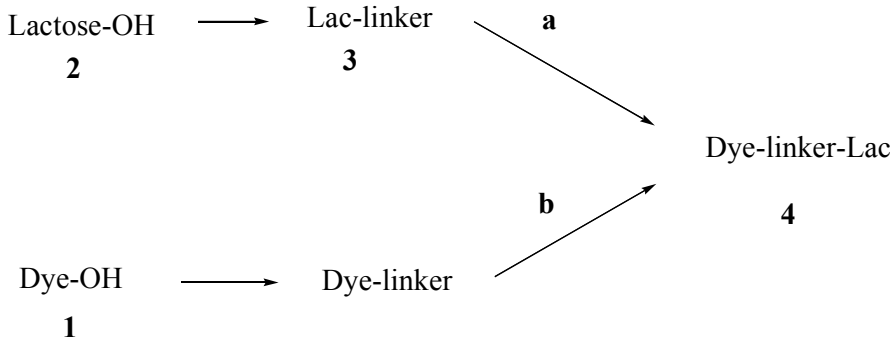

Figure 1. Schematic approach to glycoazadyes (GADs)

The study of the influence of GADs glycosidic moiety on the tinctorial properties is the aim of this research. For this purpose, protected lactose (**2**, Fig. 2), together with other protected and linked monosaccharides here not reported for brevity, have been selected in order to prepare a collection of building blocks that can be used to prepare final different GADs.

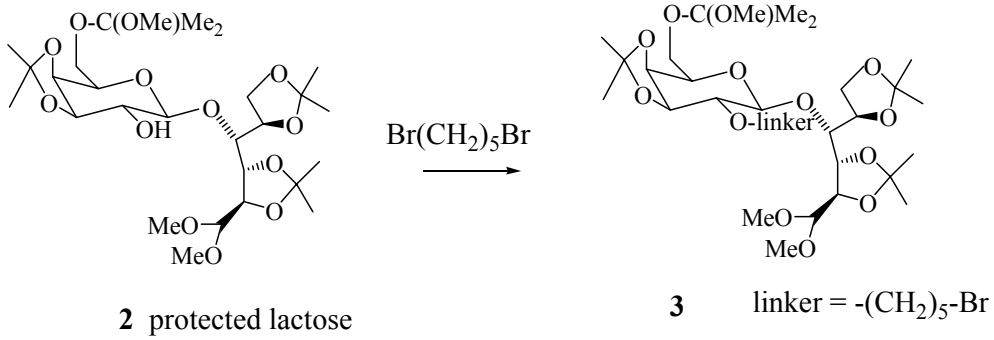

Figure 2. Protected lactose, and linked lactose

These modified glycides were used to react with a number of azadyes: Here are shown 2 of them, corresponding to the GADs of red disperse **1** (**1a** and yellow disperse 3 (**1b,** Fig. 3). Of course, products **4a** and **4b** are obtained upon final, single-step, deprotection following the coupling between the linked lactose and the dye, or the linked dye with the protected lactose but bearing a free hydroxyl in position 2'.

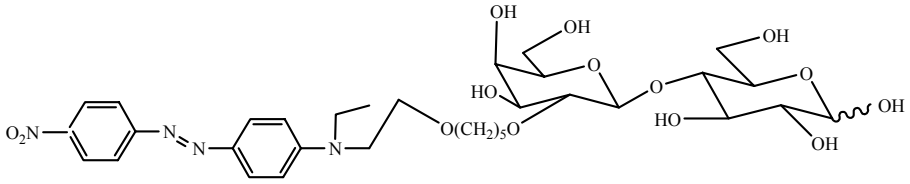

4a

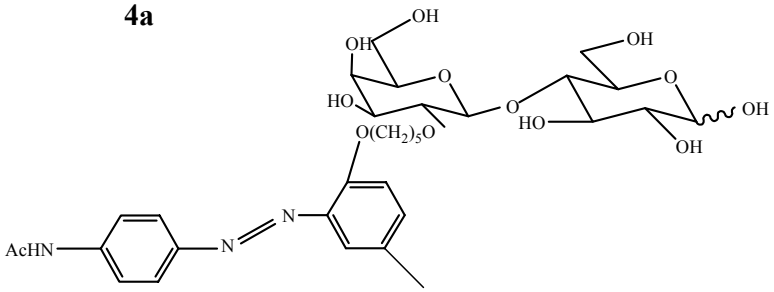

4b

Figure 3. list of modified dyes

Tinctorial Tests

Preliminary tinctorial studies were carried out on these GADs, and some of the results are reported in the following tables, thanks to a collaboration with "Italvelluti" SpA Company (Montemurlo, Italy). Later these tests were confirmed and extended by the Lanartex cnc company (Montemurlo, Italy). In Table 1 are shown the conditions of dyeing with this new class of dyes, based on the conjugation with lactose.

Table 1. Dyeing with GADs

fabric	*polyester*	*cotton* step 1	*cotton* step 2	*acetate*	*wool*	*acrylic*
Temperature bath (°C)	98	80	98	84	98	98
Time (min)	30	35	15	30	20	30
Bath Ratio[1]	50/1	50/1	50/1	50/1	50/1	50/1
Dye conc. (g/l)	1,0	1,0	1,0	1,0	1,0	1,0
Acetic acid added	1%	--	---	1%	1%	2%
other	---	Na_2SO_4 (10gr/l)	Na_2CO_3 (0,5g/l)	--	$(NH_4)_2SO_4$	
Fastness[2]	4		4/5	4	3	3/4[2]

[1]mL of water/fabric(g)
[2]washing and scraping fastness

The first evidence consists in the 'multipurposity' that characterizes now the initial aza-dye, that is a disperse dye in origin. But, as a matter of fact, when the naturalization process is carried out, through the glycoconjugation with lactose, the original dye becomes able to dye extremely different fabrics, extending from natural to artificial and synthetic ones. Moreover, the conditions applied for the dyeing processes are extremely mild and easy, especially, for example, upon considering the conditions for polyester. Polyester can be dyed with these GADs in basic conditions, not only using an acidic medium, as usual, and at a temperature near the water boiling point, but far from the 130 °C used for this fabric. Finally, no surface-active agent is added, as reported in the table, which is an evident environmental advantage. Let's consider the last row. The fastness obtained for each fabric can be considered as the evidence that the dyeing is not a lacquering, but it is in fact a proper dyeing, with good results. Also, here we are reporting on the tristimulus values for each dye and fabrics, so that the colours are well defined in the coordinates of luminosity, chromaticity, and tone, as we can see from Table 2. These tabulated values can be considered as a clear-cut demonstration that dyeing works with natutalized dyes, and that this is now an open research space for textile innovation.

Table 2- Tristimulus values for tissues dyed with GADs

Champion	*material*	*luminosity*	*Chromaticity*	*Tune*
4a	Wool	53,936	39,920	32,778
4a	Nylon[1]	42,816	61,373	43,612
4a	Acetate[1]	43,921	65,709	41,513
4a	Cotton	66,850	26,393	27,380
4a	Polyester[2]	62,126	46,993	29,776
4a	Polyester[3]	71,917	32,502	32,430
4b	Wool	74,075	47,630	85,632
4b	Nylon[1]	76,454	65,012	85,532
4b	Acetate	73,584	76,054	89,939
4b	Polyester[1]	78,994	60,524	82,505

[1]values read on a multi-fabric witness. [2]Dyed in a basic way (see Table 1)
[3] Dyed in a acid way.

Also we are confident that Table 3 will add important information on the quality of dyeing using these new generations of dyes. And in fact we can see that using ethereal glycoconjugated derivatives of Red (**4a**) or yellow (**4b**) dyes, we gave reflectance values at the two more significant wavelengths, and also K/S values, where K stands for the Kubelka-Munk absorption coefficient and S represents the scattering coefficient at the respective wavelength. Of course where we have high values of reflectance the absorption is low, and scattering is high, and viceversa.

Table 3- Reflectance and K/S Values of Fabrics Dyed with GADs **4a** and **4b**

4a					**4b**			
febric	R% (500 nm)	R% (700 nm)	K/S (500 nm)	K/S (700 nm)	R% (450nm)	R% (700nm)	K/S (450 nm)	K/S (700 nm)
wool	8	63	7,5	0,2	12	60	2,5	0,1
Nylon	5	65	9,5	0,1	10	63	5,5	0
Acetate	12	75	3,7	0,0	2	55	15	0
Cotton	20	72	1,7	0,1				
Polyester[1]	20	1,6	1,6	0,2	10	72	3,9	0

[1]Dyed in basic conditions (see Table 1)

We think that these data can be considered as a demonstration that environmentally compatible naturalized dyes can work appreciably well in the dyeing processes. The tests showed that these generations of GADs are soluble in water, as expected, and also that these dyes are multipurpose, since they dyed all of the fabrics so far tested. The results of some of these tests are reported in Fig 1. In this case the polyester has been dyed according to the basic procedure reported in Table 1. As far as we know this is the first time that a dye, which is in principle a disperse dye, at the end of story is able to directly dye wool and polyester under mild conditions. These tests, and many others not reported here, since they are covered by a deposited patent, or others on the way, have been carried out under standard conditions and were performed in water without the addition of surfactants, under mild conditions of temperature and pressure. Dispersed dyes, such as the starting azadyes, do not effectively dye wool, and they dye polyester only under drastic conditions (such as high temperature or pressure).

Figure 1. Polyester (upper row) and wool (lower row) dyed with **4a** (left) and **4b** (right).

CONCLUSIONS

A naturalization of industrial commercial dyes has been proposed, in order to maintain their good properties and improve their applications to various textiles. The synthetic modifications applied have brought:

- a higher hydrophilicity of dyes through their glycoconjugation, so that the trial dyeing processes have been carried out without the use of surfactants, or other potential pollutants;
- easier dyeing processes, avoiding high temperatures and high pressures;
- better affinity towards textiles, improving efficacy and reducing waste;
- multipurpose dyes able to dye different fabrics (synthetic, natural, artificial);

- the utilization of carbohydrates largely and cheaply available such as D-glucose, D galactose and lactose; normally discarded in huge quantities in the environment, with not negligible impact;
- new possibilities for efficient and more selective waste treatment by using, for instance, live micro-organisms to attack the sugar moiety and consequently the covalently bonded chromophore, or the use of enzymes able to destroy dyes.

ACKNOWLEDGMENTS

We thank Italvelluti SpA and Lanartex CNC companies, Montemurlo (Prato), and Cassa di Risparmio di Firenze for financial support.

This contribution was an original presentation at the *ITALIC 4 Science & Technology of Biomass: Advances and Challenges* Conference that was held in Rome, Italy (May 8-10, 2007) and sponsored by Tor Vergata University. The authors gratefully acknowledge the efforts of the Conference Organizers, Prof. Claudia Crestini (Tor Vergata University, Rome, Italy), Chair, and Prof. Marco Orlandi (Biococca University, Milan, Italy), Co-Chair. Prof. Crestini also is Editor for the conference collection issue to be published in *BioResources.*

REFERENCES CITED

Barili, P. L., Catelani, G., D'Andrea, F., De Rensis, F., and Falcini, P. (1997). "Improved preparation of 2,3:5,6:3′,4′-tri-O-isopropylidenelactose dimethyl acetal and its 6′-O-(1- methoxy-1-methylethyl) derivative," *Carbohydr. Res.* 298, 75-84.

Bartalucci, G., Bianchini, R., Catelani, G., D'Andrea, F., and Guazzelli, L. (2007). "Naturalized dyes: a simple straightforward synthetic route to a new class of dyes – glycoazadyes (GADs)" *Eur. J. Org. Chem.* 588-595.

Bianchini, R., Bartalucci, G., Catelani, G., and Seu, G. (2004). "Coloring agent containing a mono- or disaccharide"*European Pat. Appl*. no. 04005253.4, deposit 03/05/2004.

Bianchini, R., Calucci, L., Lubello, L., and Pinzino, C. (2002). "Intermediate free radicals in the oxidation of wastewaters" *Res. Chem. Intermed.* 28*,* 247-256.

Bianchini, R., Catelani, G., Cecconi, R., D'Andrea, F., Guazzelli, L., Isaad, J., and Massimo Rolla, M. (2007)."Ethereal glycoconjugated azodyes (GADs), a new group of water solubile, naturalized dyes," accepted for publication on *European Journal of Organic Chemistry*.

Bock, K., and Pedersen, C. (1983). "Carbon-13 nuclear magnetic resonance spectroscopy of monosaccharides" *Adv. Carbohydr. Chem. Biochem.* 41, 27-66.

Mascolo, G., Lopez, A., Bozzi, A., and Tiravanti, G. (2002). "By-products formation during the ozonation of the reactive dye Uniblu-A [Uniblue A]" *Ozone-Science & Engeneering* 24(6), 439-466.

Neamtu, M., Siminiceanu, I., Yediler, A., and Kettrup, A. (2002). "Kinetics of decolorization and mineralization of reactive azo dyes in aqueous solution by the UV/H_2O_2 oxidation," *Dyes and Pigments* 53, 93-99.

Perrin, D. D., Armarengo, W. L. F., and Perrin, D. R. (1980). *Purification of Laboratory Chemicals*, 2nd Ed., Pergamon Press, Oxford.

Pierce, C. I., Lloyd, J. R., and Guthrie, J. T. (2003). "The removal of colour from textile wastewater using whole bacterial cells" *Dyes and Pigments* 58*,* 179-196.

Podsiadły, R., Sokołowska, J., Marcinek, A., Zielonka, J., Chrześcijańska, E., and Socha, A. (2003) "Electrochemical and photochemical reduction of a series of azobenzene dyes in protic and aprotic solvents" *Coloration Technology* 119, 269-274.

Poon, C. S., Huang, Q., and Fung, P. C. (1999). "Degradation kinetics of cuprophenyl yellow RL by UV/H_2O_2/ultrasonication (US) process in aqueous solution" *Chemosphere* 38, 1005-1014.

Rott, U., and Minke, R. (1999)." Overview of wastewater treatment and recycling in the textile processing industry" *Water Sci. Technol.* 40, 137-144.

Selcuk, H. (2005). "Decolorization and detoxification of textile wastewater by ozonation and coagulation processes" *Dyes and Pigments* 64, 217-22.

Article received by journal: July 27, 2007; First round of peer-review completed: Sept. 16, 2007; Revised version received and accepted: Oct. 15, 2007; Article published Oct. 17, 2007.

FAST PYROLYSIS – EFFECT OF WOOD DRYING ON THE YIELD AND PROPERTIES OF BIO-OIL

Galina Dobele,[a]* Igors Urbanovich,[a] Aleksandr Volpert,[a] Valdis Kampars,[b] and Eriks Samulis[c]

The composition and properties of the products of fast pyrolysis of hardwood, obtained in a two-chamber (drying and pyrolytic) ablation type reactor in the temperature range 450-600ºC, were investigated. It has been found that, upon the additional drying of wood at 200ºC and subsequent pyrolysis, the quality of bio-oil is improved owing to the decrease in the amount of water and acids. It has been shown that the increase of the drying temperature to 240ºC decreases the yield of the main product. Optimum parameters of the drying conditions and the temperature of the pyrolysis of wood, at which the bio-oil yield exceeds 60% and its calorific value makes up 17-20 MJ/kg, have been determined.

Keywords: Pyrolytic oil, Wood, Fast pyrolysis, Drying, Ablation type reactor

Contact information: a: Latvian State Institute of Wood Chemistry, 27 Dzerbenes St., Riga, LV-100 Latvia; b: Riga Technical University, Faculty of Material Science and Applied Chemistry, 14/24 Azenes St., Riga, LV-1048, Latvia; c: Joint-Stock Company "Kņavas granulas", Kņava, Rezekne district, LV-4650, Latvia.
**Corresponding author: gdobele@edi.lv*

INTRODUCTION

The annual world's stock of plant biomass increases by 117 billion tons (in terms of the weight of oven dry material), including by 80 billion tons in forests, which is equivalent to 40 billion tons of petroleum (Zaykov 2002).

The application of renewable plant biomass resources for energy production is becoming increasingly urgent worldwide, because it becomes evident that the sources of fossil fuel energy can be exhausted dramatically with increasing industrial, transport, and agricultural outputs. As resources, low-grade wood and other forms of biomes, for example, peat, straw and bark may be used. One of the methods for utilizing waste wood for energy purposes is thermal processing.

Along this line, technologies for fast pyrolysis of wood are progressing rapidly, which enables the conversion of solid wood biomass into a liquid product – bio-oil, which can be used as a fuel or as a raw material for producing valuable chemicals. As a fuel, bio-oil is neutral with respect to the release of carbon dioxide. Upon its burning, a low amount of nitrogen oxide is released, and no sulphur dioxides are formed. Bio-oil can be stored, pumped over, and transported in the same manner as petroleum products. However, its corrosive activity (pH 2.0-2.5), high viscosity, and possible stratification, which depend strongly on temperature, should be taken into account (Bridgwater 1999). Bio-oil can be burned directly in boilers, gas turbines, and diesel engines for heat and power supply (Bridgwater et al. 2001; Czernik and Bridgwater 2005).

The composition of pyrolysis oil is similar to the biomass composition. In comparison with wood, it has a somewhat higher heat capacity, namely, 15-20 MJ/kg. The products' composition depends on the pyrolysis conditions and the wood type. Pyrolytic oils, in comparison with other fuel oils, have a similar density and a low content of ash elements (Oasmaa and Meier 2002).

In realizing the fast pyrolysis of wood, a raw material with the water content 8-10% is commonly used (Oasmaa and Meier 2002). However, the water content in pyrolytic oil is equal to 25% on average, as it includes pyroligneous water, which is formed mainly upon the dehydration of carbohydrates. The high content of water in bio-oil has an adverse effect on the calorific value of the end product. To decrease the amount of water in bio-oil, wood with a low moisture content should be used for pyrolysis. However, the temperature range of wood drying is limited by the possibility of the development of thermal-oxidative reactions, which lead to a more cross-linked condensed system of components and a higher thermal stability of the wood complex (Domburg et al. 1980).

The objective of the present work was to investigate the effect of the drying process parameters and subsequent fast pyrolysis of hardwood on the properties, chemical composition and yield of bio-oil.

EXPERIMENTAL

Raw Materials

Mixed hardwood chips (fraction 0.1-1.0 mm, moisture 8.5-9%) were used.

Pyrolysis

Fast pyrolysis was carried out using a two-chamber pyrolytic laboratory device that allows changing of the pyrolysis and drying temperatures and the duration of drying. The program "Maple10" was used for plotting the dependencies, based on multiple regression analysis.

The equipment's capacity was 150 g of the raw material in one cycle. The main constituent parts of the reactor (Fig. 1) are as follows:

- A drying chamber with a mixer and an autonomous heating and temperature control system (1).
- A pyrolysis chamber with a mixer, and an autonomous heating and temperature control system (2). The main constituent part of the pyrolysis chamber is a pan, which is heated to a definite temperature (450-700ºC). When opening a hatch, which connects chambers 1 and 2, the wood particles get onto the heated surface of the pan, where pyrolysis proceeds within 30 sec in an atmosphere of the gases formed.
- The volatile products' cooling and condensation systems (3). Condensation proceeds using a water cooling system, which consists of 2 coolers and a collector.
- Char collector.

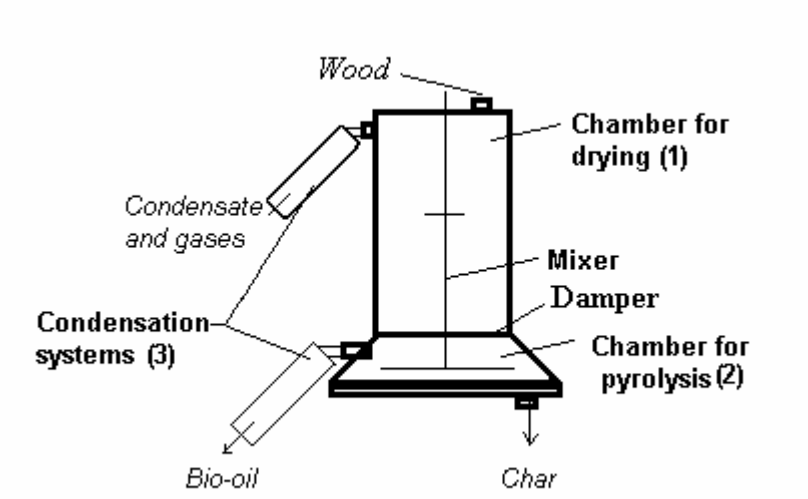

Figure 1. Schematic diagram of the laboratory pyrolytic device.

Gas Chromatography – Mass Spectrometry (GC-MS)

The pyrolytic oil was characterized with a Shimadzu GC/MS – QP 2010, capillary column RTX-1701, 60 m x 0.25 mm x 0.25 μm film. The injector temperature was 250°C, and the ion source was 250ºC with EI of 70 eV. The MS scan range was m/z 15-350. The carrier gas was helium at a flow rate of 1 ml min^{-1}, and the split ratio was 1:30. The oven program was 1 min isothermal at 60ºC, then 6ºC/min to 270ºC, and finally 10 min at 270ºC. The mass spectral database Library MS NIST 147.LI13 was used, and authentic reference compounds were found for substance identification.

Water Content in Bio-oil

A titrator Karl Fischer-270, and solution HYDRONAL-Conlomat AG were used.

Heat Capacity

Heat capacity was determined in compliance with ISO 1928-76, using an Oxygen Bomb Calorimeter-1341.

RESULTS AND DISCUSSION

To investigate the influence of drying conditions of wood, the sample was heated in the upper chamber of the reactor (1) at the temperature 200°C during 90 min, and the volatile products were cooled and condensed (Fig. 1). The results of the analysis have shown that the main component of the condensate is water, whose relative content

according to GCMS data is 80% (Table 1). Acids, ketones, and furans were present in the condensate. Among monomeric compounds, acetic acid, hydroxipropanone, and furfural were found in major amounts. The formation of these compounds is typical for low-temperature degradation of wood hemicelluloses (Kislitsin 1990).

To study the effect of wood drying on the composition of bio-oil, pyrolysis was carried out at 550°C, using wood samples with the moisture content 8.5-9% and with drying at 200°C during 90 min. The bio-oils obtained as a result of pyrolysis were analysed by GCMS. The results show that the relative content of water in the composition of the bio-oil obtained upon pyrolysis of dried wood decreased by 7.6% (Table 1). Besides, the content of acids decreased mainly at the expense of acetic acid, and the content of compounds with carbonyl groups and anhydrosaccharides increased.

Table 1. Chemical Composition of Volatile Products, Obtained upon Drying and Pyrolysis of Wood (relative content from GCMS, %)

Compounds	Content in volatile products, relative %		
	Drying (200°C, 90 min)	Pyrolysis (550°C)	Drying (200°C, 90 min) and pyrolysis (550°C)
H_2O	80.1	22.0	14.4
Acids, Esters	11.6	20.2	17.8
Alcohols, Aldehydes	0.9	9.3	11.9
Ketones, Lactones	3.1	15.0	16.0
Pyrans	0.0	1.5	1.5
Furans	1.7	6.6	7.4
Levoglucosan	0.0	1.6	3.7
Phenols, lignin derivatives	0.8	23.5	24.2

The amount of water in bio-oil, determined by titration according to the Fischer method, decreased to 19-20% upon pyrolysis of dried wood in comparison with the 25-28% in bio-oil, obtained upon pyrolysis of a moist wood sample (Table 2).

The results of the analysis of the heat capacity of pyrolytic oils showed an increase in this parameter from 14 MJ/kg (without drying) to 17-20 MJ/kg, when the wood was dried and then pyrolysed (Table 2). Obviously, the main factor that influences this parameter is the decrease in the amount of water in the bio-oil.

An increase in pH (Table 2) during the two-stage process has been observed. It can be explained by the release of acetic acid in the first stage of the process. This factor is very important, taking into account the high corrosive activity of pyrolytic oils, which also determines the required construction material of the reactor.

Table 2. Properties of pyrolytic oil*

Characteristics	Pyrolysis at 550°C	
	Without drying	Drying at 200°C, 90 min
Heat capacity, MJ/kg	14	17-20
Water amount, %	25-28	19-20
pH	2.3 –2.5	3.0-3.2
Bio-oil yield, %	62-64	63

* 4 replicates of experiments were made

To elucidate the effect of the temperature and duration of drying on the yield of liquid, solid, and gaseous products, pyrolysis of wood dried at different temperatures was carried out (Figs. 2, 3).

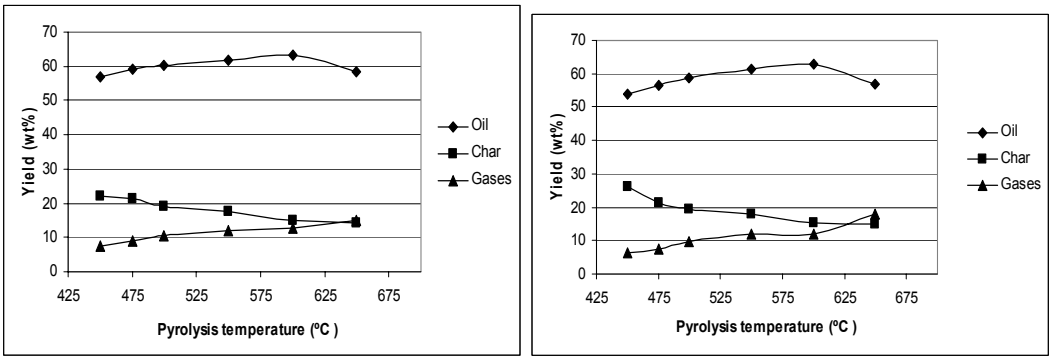

Figure 2. Change in the yield of oil, char and gases *versus* the temperature of pyrolysis of wood (drying temperature 200ºC (a) 45 min, (b) 90 min).

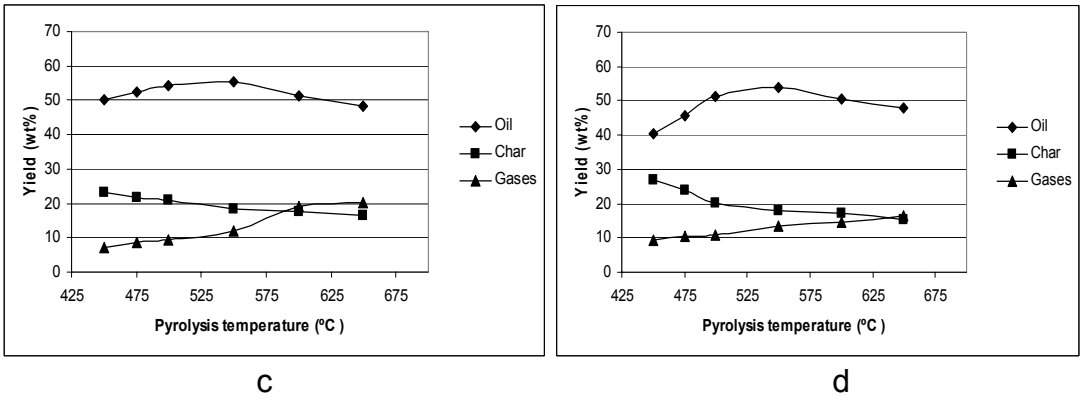

Figure 3. Change in the yield of oil, char and gases *versus* the temperature of pyrolysis of wood (drying temperature 240ºC (c) 45 min and (d) 90 min).

The results of the pyrolysis of wood samples, dried at temperatures of 200 and 240ºC, have shown that the increase in the drying temperature influenced the yield of pyrolysis products, while the increase in the drying time from 45 to 90 min did not affect it (Figs. 2 (a, b), 3 (c, d)). Upon pyrolysis of the wood dried at 200ºC, the bio-oil yield grew with increasing temperature from 450ºC to 600ºC, reaching 63% (Fig. 2 (a, b)). Further rise in temperature led to a decrease in the bio-oil yield and an increase in the amount of non-condensing gases.

Upon pyrolysis in the temperature range 450-650ºC of wood samples, whose drying was performed at 240ºC (Fig. 3 (c, d)), the bio-oil yield was lower. Its maximum value was reached at a lower temperature, in comparison with the case of the samples dried at 200ºC. At increasing pyrolysis temperature above 550ºC, no additional amount of liquid products was formed. Obviously, upon drying of wood at 240ºC, the formation of new, thermally more stable bonds occurs (Chirkova et al. 2006), which results also in

a higher yield of the char residue and an increase in the amount of non-condensing gases upon pyrolysis of these samples.

The results of modelling of the pyrolysis process show that the yield of pyrolytic oil changed upon varying both drying temperature and pyrolysis temperature (Fig. 4). The optimum conditions for the formation of bio-oil were a drying temperature of 200°C and a pyrolysis temperature of 550°C. The maximum yield of bio-oil was 63% of the dry raw material. The decrease in the drying temperature below the optimum level influenced the bio-oil yield only insignificantly.

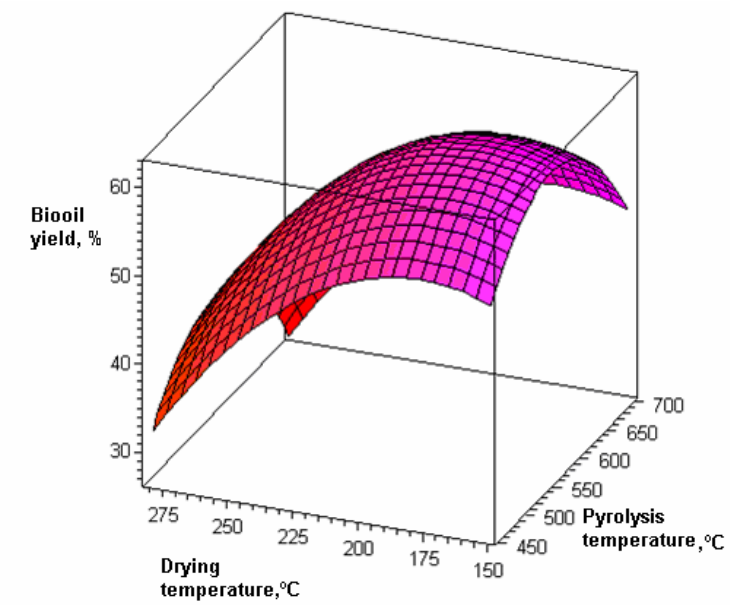

Figure 4. Change in the yield of bio-oil upon pyrolysis of wood *versus* the temperature of drying and pyrolysis (drying time 90 min).

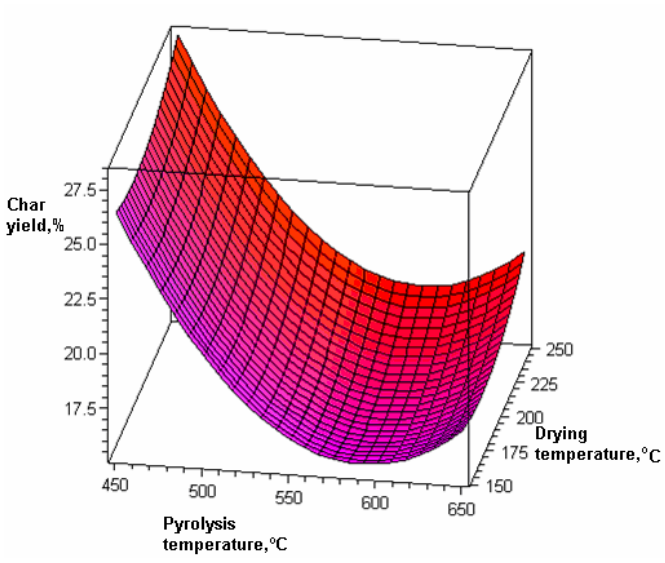

Figure 5. Change in the yield of char upon pyrolysis of wood *versus* the temperature of drying and pyrolysis (drying time 90 min).

At the same time, the increase in the drying temperature and the changes in the pyrolysis temperature below and above the optimum levels had an equal adverse action on the bio-oil yield. The latter decreased and reached about 40% at the drying temperature 275°C.

The drying temperature practically did not influence the formation of char (Fig. 5).

The lowest quantity of char was formed under pyrolysis conditions that were optimum for obtaining bio-oil. At a temperature of 450°C, the char yield was the highest, namely, 27%.

CONCLUSIONS

1. The process of fast pyrolysis of hardwood using a two-chamber ablation type reactor has been investigated, depending on the drying conditions and pyrolysis temperature.
2. It has been found that the drying of the raw material at 200ºC and pyrolysis at 550ºC resulted in improving of the quality of bio-oil. The improvements included a decrease in the water content to 19-20%, increased pH, and a calorific value of 17-20 MJ/kg.
3. It has been found that the drying of wood at the temperature 240ºC obviously led to condensation reactions and cross-linking of wood components, as well as a decrease in the yield of bio-oil.
4. The maximum yield of bio-oil (above 60%) was obtained under the conditions of drying at 200ºC and pyrolysis at 550ºC. The lowest quantity of char was formed under pyrolysis conditions that were the optimum for obtaining bio-oil.
5. Drying of wood at a higher temperature (above 200°C) decreased the yield of liquid products of pyrolysis.

ACKNOWLEDGEMENTS

This work has been partly supported by the European Social Fund within the National Programme "Support for carrying out doctoral study programmes and post-doctoral researches" project "Support for the development of doctoral studies at Riga Technical University", Latvian Grant N1273 and Latvian National Programme part N8113.

REFERENCES CITED

Bridgwater, A. (1999). "An introduction to fast pyrolysis of biomass for fuels and chemicals," *Fast Pyrolysis of Biomass: A Handbook,* (1) CPL Press, UK, 1-13.

Bridgwater, A., Czernik, S., and Piskorz, J. (2001). "An overview of fast pyrolysis," *Progress in Thermochemical Biomass Conversion*, Bridgwater (ed.), Blackwell Science, London, UK, 977-997.

Chirkova, J., Dobele, G., Urbanovich, I., Andersone, I., and Andersons, B. (2006). "Structural and chemical changes in wood and lignin at low temperature treatment," *Proc. European Workshop on Lignocellulosics and Pulp*, August 27-30, 2006, 196-199.

Czernik, S., and Bridgwater, A. (2005). "Applications of biomass fast pyrolysis oil," *Fast Pyrolysis of Biomass: A Handbook*, (3) CPL Press, UK, 105-120.

Domburg, G., Sharapova, T., and Scripchenko, T. (1980). "Besonderheiten der thermischen Zersetzung von Lignin in Cellulose enthaltenden Komplexen," *Zellstoff und Papier*, 3, 129-131.

Kislitsin, A. (1990). "Pyrolysis of wood: chemical activity, kinetics, products, new processes," *Lesnaja Promyshlennost'*, Moscow, 313 p. (in Russian).

Oasmaa, A., and Meier, D. (2002). "Analysis, characterisation and test methods of fast pyrolysis liquids," *Fast Pyrolysis of Biomass: A Handbook,* (2) CPL Press, UK, 23-35.

Oasmaa, A., and Meier, D. (2002). "Pyrolysis liquids analyses: The results of IEA-EU round robin," *Fast Pyrolysis of Biomass: A Handbook,* (2) CPL Press, UK, 41-58.

Oasmaa, A., Peacocke, C., Gust, S., Meier, D., and McLellan, R. (2005). "Norms and standards for pyrolysis liquids," *Energy and Fuels* 19(5), 2155-2163.

Zaykov, G. (2002). "Chemistry and provision of mankind with energy," *Nauka I Tehnika (Science and Engineering),* 12, 35-40 (in Russian).

Article submitted: July 17, 2007; First round of peer-reviewing completed: Sept. 11, 2007; Revision received: Oct. 12, 2007; Article accepted: Oct. 26, 2007; Published: Oct. 28, 2007

RADICAL FORMATION ON TMP FIBERS AND RELATED LIGNIN CHEMICAL CHANGES

Luca Zoia,[a] Carmen Canevali,[b*] Marco Orlandi,[a] Eeva-Liisa Tolppa,[a] Jussi Sipila,[c] and Franca Morazzoni[b]

Oxidation of TMP fibers was compared at 298 K with molecular oxygen, in the presence of either [Co(salen)] in methanol or [Co(sulphosalen)] in water. Electron paramagnetic resonance (EPR) spectroscopy made it possible to reveal and quantify the formation of phenoxy cobalt radicals in the former case and of phenoxy radicals in the latter. These radicals reached the same concentration after 60 min from the onset of reaction. Fiber integrity was more preserved after oxidation in water than in methanol, as assessed by heteronuclear single quantum coherence - nuclear magnetic resonance (2D-HSQC-NMR) spectroscopy, nuclear magnetic resonance spectroscopy of carbon (^{13}C-NMR), and Gel Permeation Chromatography (GPC). These results suggest that efficient radical formation on fibers can be achieved also with water-soluble catalysts. Thus, it is proposed that treatment with molecular oxygen in the presence of [Co(sulphosalen)] in water represents a promising way to approach an environmentally sustainable radicalization of fibers, without heavy modification of the lignin structure.

Keywords: Lignocellulosic fibers, Phenols, [Co(salen)], [Co(sulphosalen)], Radicals, EPR, NMR

*Contact information: a: Dipartimento di Scienze dell'Ambiente e del Territorio, Università di Milano-Bicocca, Piazza della Scienza 1, 20126 Milano, Italy; b: Dipartimento di Scienza dei Materiali, Università di Milano-Bicocca, Via R. Cozzi 53, 20125 Milano, Italy; c: Laboratory of Organic Chemistry, University of Helsinki, P.O. Box 55 FIN-00014, Helsinki, Finland; *Corresponding author: carmen.canevali@unimib.it*

INTRODUCTION

In the field of packaging, materials with high barrier and mechanical properties are generally required. Wood fibers can achieve these properties, after proper modification. Attempts to modify fiber properties by grafting synthetic polymers onto the cellulose backbone started as early as the 1940´s. Radical centers at the cellulose backbone behave as grafting initiators, and they can be generated by high-energy irradiation, by oxygen reaction in the presence of transition metal complexes, by decomposition of peroxides, or by radical transfer reaction (Bledzki et al. 1998). Alternatively, radical active centers can be produced on lignin at the fiber surface. As an example, the reaction of wood fibers obtained from thermomechanical pulp (TMP) with molecular oxygen and laccase as catalyst, was demonstrated to produce the radicalic activation of the surface lignin phenols through the formation of phenoxy radicals (Lund et al. 2003):

$$4\ PhOH + O_2 \xrightarrow{\text{laccase}} 4\ PhO^{\bullet} + 2\ H_2O \quad (1)$$

Under such treatment, glueless fiberboards were obtained, and the wet strength of paper was improved (Felby et al. 1997a; Lund and Felby 2001). The radical formation from surface lignin phenols can also improve other properties of interest for specific applications, such as hydrophobic or hydrophilic character (Buchert et al. 2005), as well as the improvement of paper strength properties (Chandra et al. 2004).

Besides by enzymatic treatment, phenoxy radicals on fibers can also be generated by reaction with molecular oxygen, using biomimic catalysts such as salen compounds. It was reported that molecular oxygen, in the presence of N,N'-ethylenebis-(salicylideneiminato) cobalt(II), [Co(salen)] (Scheme 1), efficiently formed radicals on CTMP and TMP fibers in methanol (Canevali et al. 2005).

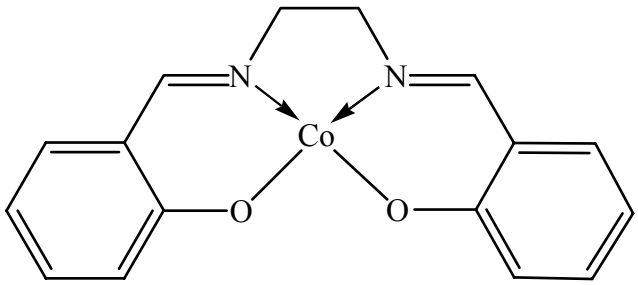

Scheme 1.

The characterization of the intermediate paramagnetic species by electron paramagnetic resonance (EPR) spectroscopy suggested that the radicalization mechanism was the same as that proposed for lignin model compounds in homogeneous phase (Bolzacchini et al. 1997; Canevali et al. 2002), occurring through the following three steps:

$$[Co^{II}(salen)] + ROH + O_2 \rightleftharpoons [Co^{III}(salen)(ROH)(O_2^{-})] \quad (2)$$

$$[Co^{III}(salen)(ROH)(O_2^{-})] + ROH \rightleftharpoons [Co^{III}(salen)(ROH)(RO^{\bullet})] + HO_2^{-} \quad (3)$$

$$[Co^{III}(salen)(ROH)(RO^{\bullet})] + HO_2^{-} \rightleftharpoons [Co^{III}(salen)(RO^{-})(RO^{\bullet})] + H_2O_2 \quad (4)$$

where ROH is the phenol unit and $RO^{\bullet}$ the corresponding intermediate radical. In the first step of this mechanism, [Co(salen)] is co-ordinated by ROH and O_2, giving a superoxocobalt derivative, detected by EPR. In the second step, the superoxocobalt derivative reacts with another phenol ligand, giving an EPR active phenoxy cobalt radical, $[Co^{III}(salen)(ROH)(RO^{\bullet})]$. In the third step, the phenoxy cobalt radical is in equilibrium with a phenoxy-phenate cobalt radical; both were detected by EPR.

After treatment with molecular oxygen in methanol in the presence of [Co(salen)], TMP fibers formed a higher amount of radicals and in parallel underwent deeper structural and morphological changes than CTMP (Canevali et al. 2005). By using

[Co(salen)] as catalyst, the absolute amount of radicals in fibers reaches very high values, 10 times higher than those reported in the literature for the treatment with laccase and molecular oxygen of TMP (Felby et al. 1997b) and of milled wood lignin (Ferm et al. 1972). These results are probably due to the smaller molecular dimension of [Co(salen)] compared with laccase, which allows the biomimic catalyst to interact also with subsurface lignin phenol groups.

However, [Co(salen)] does not allow an environmentally sustainable radical formation on fibers and a water soluble catalyst should be used instead.

With the aim of developing an eco-friendly process for maximizing the radical amount, while preserving the fiber integrity, in the present paper the treatments of unbleached TMP fibers with molecular oxygen, in the presence of either [Co(salen)] in methanol or [Co(sulphosalen)] (Scheme 2) in water were compared.

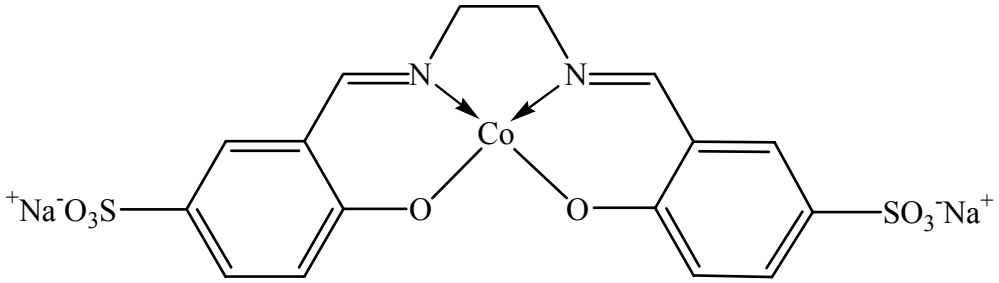

Scheme 2.

The best conditions for radical formation on TMP fibers using salen catalysts were assessed in the proper solvent by varying the reaction time, under the experimental conditions which were found to maximize the formation of radicals in the presence of [Co(salen)] (Canevali et al. 2005).

The radicals formed on fibers during oxidation were identified and quantified by EPR spectroscopy. The radical formation data were correlated to the changes in lignin chemical structure, achieved by lignin units under oxidative treatments, as assessed by heteronuclear single quantum coherence - nuclear magnetic resonance (2D-HSQC-NMR) spectroscopy, nuclear magnetic resonance spectroscopy of carbon (^{13}C-NMR) and Gel Permeation Chromatography (GPC).

EXPERIMENTAL

Materials

Pulps

The softwood unbleached thermomechanical pulp (TMP) was provided by Stora Enso Oyj. The amount of lignin in pulp was evaluated using the Klason method (Dence 1992) and resulted 27.1 %. %. The amount of extractives in pulp evaluated by Stora Enso, is reported in Table 1:

Table 1. Amounts of Extractive Components in TMP

Percentage of total extractives (w/w)	Fatty acids (mg/g)	Resin acids (mg/g)	Lignans and sterols (mg/g)	Sterylesters (mg/g)	Triglycerides (mg/g)
1.39	0.94	0.88	0.42	0.64	0.65

Reagents

N,N'-ethylenebis(salicylideneiminato) cobalt(II), [Co(salen)] (99%), was supplied by Aldrich. (Bis[(5-sulphonatosalicylaldehyde)ethylenediiminato] cobalt(II)) disodium, [Co(sulphosalen)], was synthesized according to the literature (Sippola and Krause 2003). Methanol and deuterated DMSO-d_6 (Fluka) were used as received. Mill-Q water was used. Oxygen (99.99%) was supplied by Technogas.

Methods

Radical formation on fibers

Fibers and fines, hereafter named "fibers", were obtained by suspending pulp in dichloromethane for 30 min, then in methanol for 60 min, under mechanical stirring, in order to eliminate extractives. Then, lignocellulosic fibers were recovered by filtration and dried in air at 353 K.

The best conditions for radical formation on TMP fibers using salen catalysts were assessed in the proper solvent by varying the reaction time, under the experimental conditions which were found to maximize the formation of radicals in the presence of [Co(salen)]: 298 K; fiber/[salen] ratio 10:1 w/w, corresponding to a molar ratio phenol/[salen)] ~ 0.8; fiber concentration in the solvent 5.0 mg/ml; oxygen pressure 1 bar (Canevali et al. 2005). Thus, radicals were formed by suspending fibers (150 mg) in 30 ml of either methanol containing [Co(salen)] (15 mg) or water in the presence of [Co(sulphosalen)] (15 mg), then fibers were allowed to react for the required time with molecular oxygen (1 bar pressure) at 298 K.

After reaction, fibers were recovered by filtration, washed either three times with 30 ml of ethyl acetate and three times with 20 ml of acetone (after [Co(salen)] treatment) or three times with 20 ml of water (after [Co(sulphosalen)] treatment). The washed fibers were allowed to dry in air, then subjected to spectromagnetic and structural characterization.

Solvents and washing liquids were collected in order to check the presence of paramagnetic species by EPR spectroscopy. In all cases paramagnetic species were absent in these samples.

EPR measurements

Immediately after drying in air, fibers were inserted into the EPR tube and frozen at the liquid nitrogen temperature, in order to inhibit further reaction before the spectromagnetic investigation.

The EPR spectra were recorded at 123 K on a Bruker EMX spectrometer working at the X-band frequency, equipped with a variable temperature BVT 2000 unit (Bruker).

The g values were determined by standardization with α,α'-diphenyl-β-picryl hydrazyl (DPPH). The amount of paramagnetic species, expressed as area/mg, was calculated with a ± 10 % accuracy by double integration of the resonance lines and by accurately determining the weight of dry fibers filling 1 cm length of the EPR tube (sensitive part of the EPR cavity).

NMR analyses

NMR analyses were performed on lignin extracted from TMP fibers by a modification of the acidolysis method developed in the literature (Gellerstedt et al. 1994): dried fibers (5 g) were suspended in 175 ml of dioxane/water 82:18 v/v (0.1 M HCl) and refluxed under nitrogen for 3 h. The fibers were filtered and washed 3 times with 15 ml of dioxane/water 82:18 v/v, then with distilled water to reach a neutral pH. The filtrate was then evaporated under reduced pressure at 313 K until dioxane had been removed. The aqueous solution was kept overnight in a refrigerator to induce coagulation of lignin; the precipitate was collected by filtration through a fine porous glass filter and washed with distilled water. After drying in air at 353 K for 2 h, lignin was refluxed with hexane in a Soxhlet extractor for 8 h in order to remove low molecular weight compounds. The yield of lignin, evaluated as (extracted lignin) / (lignin in pulp) w:w %, was around 35-40%.

The extracted lignin was acetylated with acetic anhydride:pyridine 1:1 v/v and each sample, approximately 60 mg, dissolved in 0.75 ml DMSO-d_6. The inverse detected ^{1}H-^{13}C correlation (2D-HSQC-NMR) spectra were recorded on a Bruker 500 MHz instrument at 308 K. The spectral width was set 5 kHz in F2 and 25 kHz in F1. Altogether 128 transients in 256 time increments were collected. The polarization transfer delay was set at the assumed coupling of 140 Hz and a relaxation delay of 2 s was used. Spectra were processed using Π/2 shifted squared sinebell functions in both dimensions before Fourier transform. The ^{1}D-^{13}C spectra were recorded using a Varian Mercury 400 MHz instrument at 308 K. The chemical shifts were referred to the solvent signal at 39.5 ppm. A relaxation delay of 10 s was used between the scans. Line broadening of 2-5 Hz was applied to FIDs before Fourier transform. For each spectrum, typically about 8000 scans were accumulated.

The number of primary, secondary and phenolic OH groups per aromatic ring was calculated (Cyr and Ritchie 1989; Faix et al. 1994; Robert and Brunow 1984; Landucci 1985) by multiplying the intensity of signals due to acetylic carboxyl groups divided by the intensity of signal due to methoxyl group, with the average number of methoxyl groups per aromatic ring in TMP lignins, this last number being evaluated by elemental and gas-chromatographic analyses (Girardin and Metche 1983).

GPC analyses

The investigation was carried out on acetylated lignin extracted from fibers. Before analysis, the acetylated lignin samples were dissolved in THF.

Analyses were performed using a Waters 600 E liquid chromatograph connected with an HP 1040 ultraviolet diode array (UV) detector set at 280 nm. The GP-column was an Agilent PL 3 μm MIXED gel E MW 220-400W. Polymer standards of poly(styrene) (PS) from Polymer Laboratories were used for calibration. The PS-

calibration curve was tested using acetylated dimeric, tetrameric, and hexameric lignin model compounds. Analysis were performed at a flow rate of 0.8 ml/min

The evaluation of both the number-average molecular weight (M_n) and the weight-average molecular weight (M_w) was performed following the methodology developed in the literature (Himmel et al. 1989).

RESULTS AND DISCUSSION

Radical Formation on Fibers

Radicals formed on TMP fibers after reaction at 298 K with molecular oxygen in the presence of either [Co(salen)] in methanol or [Co(sulphosalen)] in water, were identified and quantified by EPR spectroscopy at 123 K (see Experimental).

In water an isotropic signal (g = 2.004 ΔHpp = 9 G) was observed (Fig. 1), very similar to that formed on fibers after treatment with laccase (Hon 1992) and attributable to phenoxy radicals.

In methanol an eight-resonance line signal was detected (Fig. 2a), very similar in shape to that observed (Bolzacchini et al. 1997; Canevali et al. 2002) in frozen solution during the oxidative degradation of lignin model compounds (Fig. 2b), which is attributable to the phenoxy cobalt radical, [Co^{III}(salen)(ROH)($RO^{\bullet}$)].

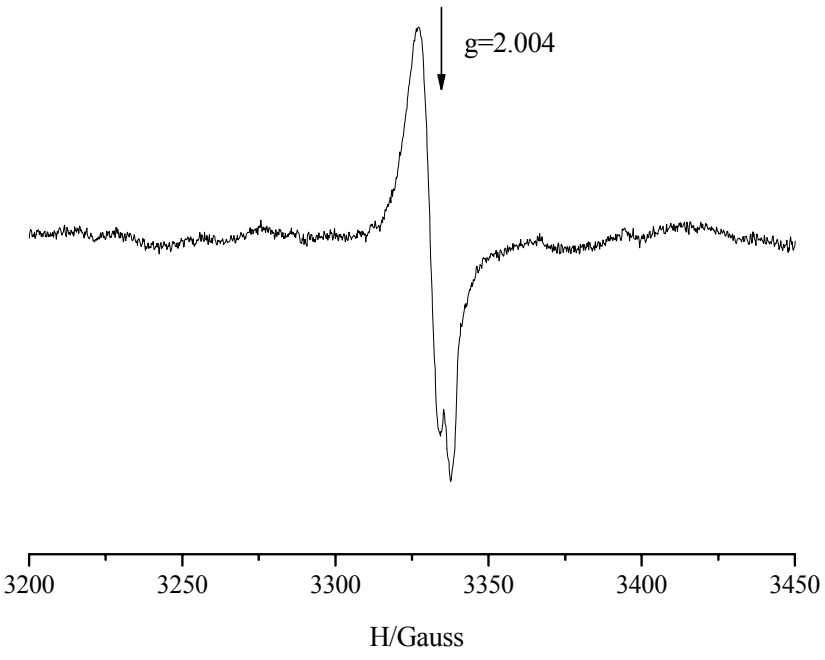

Fig. 1. X-band EPR spectrum recorded at 123 K on TMP fibers after oxidation in water in the presence of [Co(sulphosalen)] at 1 bar O_2 pressure for 60 min.

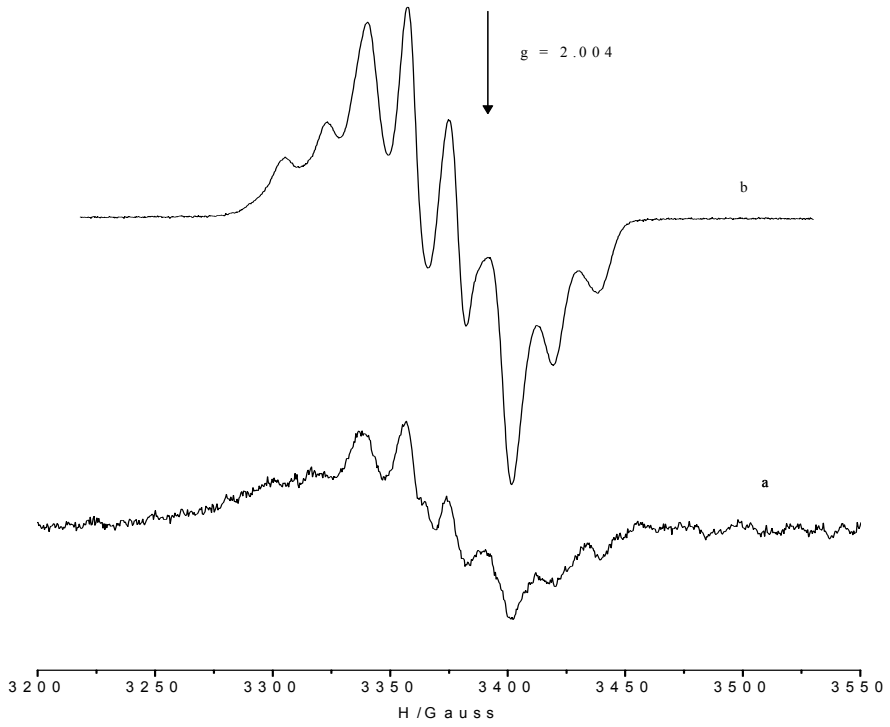

Fig. 2. X-band EPR spectra recorded at 123 K after oxidation in methanol in the presence of [Co(salen)] at 1 bar O_2 pressure for 30 min a) on TMP fibers and b) on E-methyl ferulate.

The radical signal formed by lignin model compounds in solution was deeply investigated in previous studies, both by X-band and high frequency (HF) EPR spectroscopy and showed axial magnetic anisotropy of g and A (^{59}Co) tensor components, with $g_{\perp} > g_{||}$ and $A_{||} > A_{\perp}$. The hyperfine coupling constant values vary with the ROH molecule (Canevali et al. 2002). In the case of lignocellulosic fibers, the observed signal is probably the envelope of several phenoxy cobalt radicals, which are $[Co^{III}(salen)(ROH)(RO^{\bullet})]$-like, originated by the co-ordination of [Co(salen)] to different phenols present at the lignin surface. This causes a higher width of resonance lines with respect to the species containing a unique ROH ligand (Canevali et al. 2005).

The difference in the paramagnetic species formed during oxidation in the presence of [Co(salen)] and [Co(sulphosalen)] needs further investigation in order to be explained, which goes behind the scope of the present paper.

The best conditions for radical formation on TMP were assessed by evaluating the amount of paramagnetic species formed at different times of reaction (5, 15, 30, 60 min) in the presence of [Co(sulphosalen)] in water (Fig. 3a) or in the presence of [Co(salen)] in methanol (Fig. 3b).

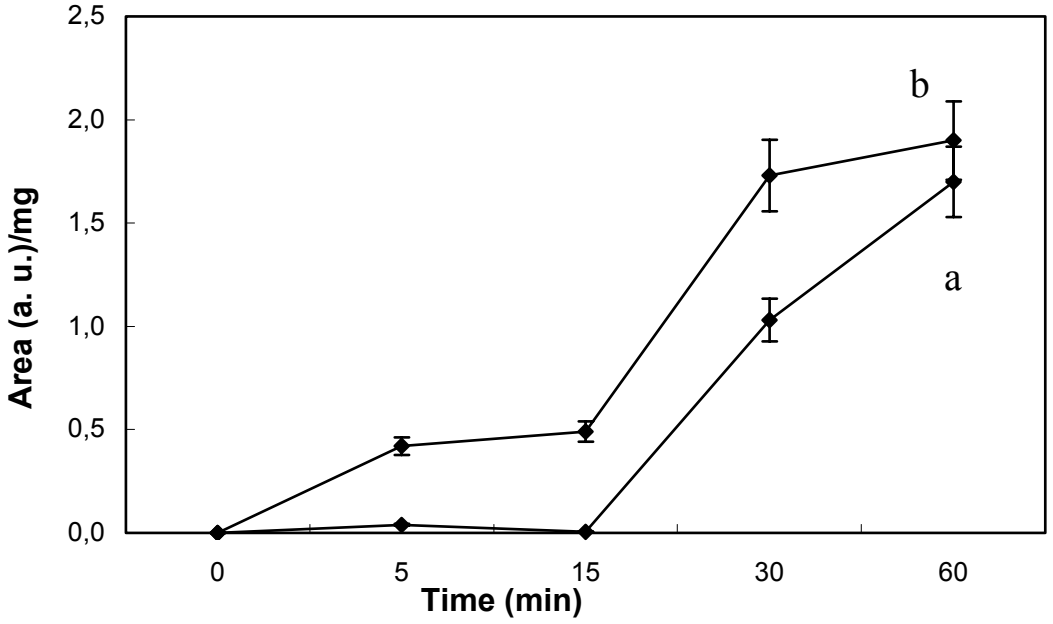

Fig. 3. Amounts of radicals, reported as area of EPR resonance lines (arbitrary units) per TMP fiber weight (mg), formed at different reaction times: a) phenoxy radicals formed in the presence of [Co(sulphosalen)] in water and b) phenoxy cobalt radicals formed in the presence of [Co(salen)] in methanol.

During both treatments, the amount of radicals gradually increased, [Co(salen)] in methanol being more reactive than [Co(sulphosalen)] in water at each time of reaction, except after 60 min of reaction, when the amounts of radicals formed in the two ways do not significantly differ.

Change in Lignin Structure

In order to evaluate changes in lignin chemical structure induced by catalytic oxidations in the presence of [Co(salen)] or [Co(sulphosalen)], lignins extracted by acid hydrolysis of fibers were characterized by 2D-HSQC-NMR spectroscopy, to identify the main intermonomeric units, and by ^{13}C-NMR spectroscopy, to quantify the principal intermonomeric units and the amount of alcoholic and phenolic groups. Spectra were run in DMSO-d_6 on the acetylated samples for the following three reasons: i) to avoid lignin fractionation before NMR analysis (Sipila 2002), ii) to increase the lignin solubility in DMSO-d_6 and iii) to enhance the chemical shift dispersion of the side chain units (Adler et al. 1987). As investigated lignins were obtained from both unreacted and oxidized fibers, the structure modifications due to the oxidative treatment were unequivocally distinguished from those due to the isolation method.

A preliminary evaluation by Klason method (Dence 1992) of the lignin amount in fibres after oxidation treatments and a preliminary evaluation of methoxyl content in lignin by the Zeisel method (Girardin and Metche 1983) allowed us to exclude relevant delignification effects. The data are reported in Table 2.

Table 2. Lignin Amount in TMP Fibres Before and After Treatment with [Co(salen)] and [Co(sulphosalen) and Amount of Methoxyl Content In Lignin Extracted from Fibres Before and After Treatment with [Co(salen)] and [Co(sulphosalen)].

Type of fibers	% lignin amount in fibers *	μmol OCH_3 / mg lignin**
Untreated TMP	27,1	4,06
[Co(salen)]-treated TMP	27,0	4,05
Co(sulphosalen)]-treated TMP	27,1	4,07

*Klason method, ** Zeisel method

The assignment of predominant signals in 2D-HSQC-NMR spectra was based on the chemical shift data of lignin model compounds and of milled wood lignin (MWL), as reported in the literature (Drumond et al. 1989; Ralph 1996; Kilpelainen et al. 1994). The predominant intermonomeric units found in TMP lignins extracted from fibers are reported in Scheme 3: arylglycerol-β-aryl ether (β-O-4 unit), phenylcoumaran (β-5 unit), pinoresinol (β-β unit) and dibenzodioxocine (5-5'-O-4 unit).

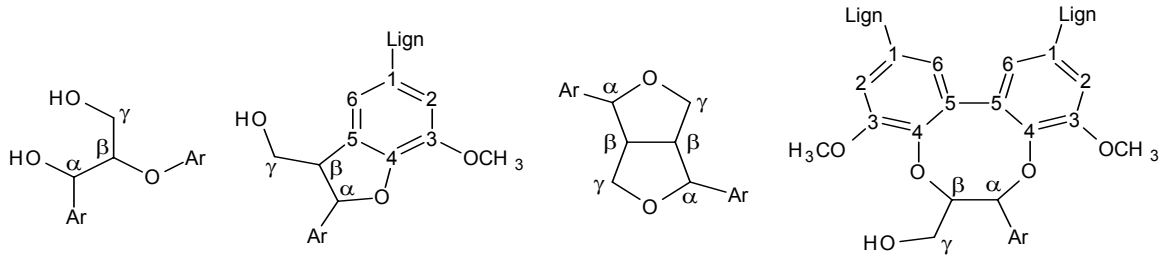

β-O-4 β-5 β-β 5-5'-O-4

Scheme 3.

The quantitative evaluation of the predominant intermonomeric units by ^{13}C-NMR showed that unreacted TMP lignin and TMP lignin treated with [Co(sulphosalen)] were rich in β-O-4 units and also contained significant amounts of β-5 units (Table 3). Instead, after [Co(salen)] treatment, the amount of β-O-4 and β-5 units in acetylated lignin approximately reduced to a half, with respect to untreated TMP. The amount of β-β units did not change after both treatments, while the 5-5'-O-4 units were not observed in lignin extracted from [Co(salen)]-treated TMP.

Table 3. Relative Amounts of the Predominant Intermonomeric Units in TMP Lignins Extracted from Fibres Before and After Treatment with [Co(salen)] and [Co(sulphosalen)].

Structural units	Untreated TMP	[Co(salen)]-treated TMP	[Co(sulphosalen)]-treated TMP
β-O-4	++++	++	+++
β-5	++	+	++
β-β	+	+	+
5-5'-O-4	+	traces	+

In addition to the elucidation of the structural changes in lignin intermonomeric composition, a quantitative evaluation of alcoholic and phenolic groups in TMP fibers, before and after the oxidative treatments, was also performed. It was shown that treatment in the presence of [Co(salen)] induced significant changes in the amount of alcoholic and phenolic groups per aromatic ring, while in the presence of [Co(sulphosalen)] the number of hydroxyl groups did not significantly change (Table 4). These results agree with the observed relative amounts of the predominant intermonomeric units, detected by ^{13}C-NMR and suggest that chemical lignin structure is better preserved after treatment with [Co(sulphosalen)] in water than with [Co(salen)] in methanol.

Table 4. Number of Primary, Secondary and Phenolic OH per Aromatic Ring in TMP Acetylated Lignins, Before and After Treatment with [Co(salen)] and [Co(sulphosalen)].

OH Type/C_6H_6	δ/ppm	Untreated TMP	[Co(salen)]-treated TMP	[Co(sulphosalen)]-treated TMP
primary	169.9-171.0	0.52	0.36	0.52
secondary	169.5	0.28	0.24	0.29
phenolic	168.6	0.20	0.15	0.19

The effects of salen treatments on lignin structure were also elucidated by evaluating the molecular weight distribution changes in the extracted acetylated lignins. Results show that the changes in M_n, M_w and polydispersity (M_w/M_n) of acetylated lignins, after [Co(sulphosalen)] treatment, are not significant, whereas in the case of [Co(salen)] treatment a small increase for M_n (from 5600 to 7500) and for M_w (from 13600 to 18000) was observed (Table 5). These results agree with those obtained by NMR investigation.

Table 5. M_n, M_w and Polydispersity Ratio (M_w/M_n) Values of TMP Acetylated Lignins, Before and After Treatment with [Co(salen)] and [Co(sulphosalen)].

Molecular weight distribution	Untreated TMP	[Co(salen)]-treated TMP	[Co(sulphosalen)]-treated TMP
M_n	5600 ± 500	7500 ± 500	5800 ± 500
M_w	13600 ± 1000	18000 ± 1000	14100 ± 1000
M_w/M_n	2.43 ± 0.04	2.40 ± 0.04	2.43 ± 0.04

CONCLUSIONS

1. The results of EPR investigation showed that the oxidation of unbleached TMP fibers by molecular oxygen, catalyzed by [Co(sulphosalen)] in water, induced the formation of phenoxy radicals that were very similar to those reported in the literature for the treatment of the same fibers with molecular oxygen and laccase (Lund et al. 2003). By contrast, in the presence of [Co(salen)] in methanol, phenoxy cobalt radicals similar in structure to those formed during the oxidation of lignin model compounds (Bolzacchini et al. 1997; Canevali et al. 2002) were observed.
2. After 60 min of reaction, the amount of radicals formed on TMP fibers in the presence of either [Co(salen)] or [Co(sulphosalen)] did not significantly differ. This result suggests that that efficient radical formation on fibers can be achieved also with water-soluble catalysts
3. The modification of lignin chemical structure was lower after oxidation with [Co(sulphosalen)] in water than with [Co(salen)] in methanol, as assessed by 2D-HSQC-NMR, ^{13}C-NMR and GPC.
4. The obtained results showed that the treatment with molecular oxygen in the presence of [Co(sulphosalen)] in water represents a promising way to approach an environmentally sustainable radical formation on fibers, without an heavy modification of the lignin structure.

ACKNOWLEDGMENTS

This contribution was an original presentation at the *ITALIC 4 Science & Technology of Biomass: Advances and Challenges* Conference that was held in Rome, Italy (May 8-10, 2007) and sponsored by Tor Vergata University. The authors gratefully acknowledge the efforts of the Conference Organizers, Prof. Claudia Crestini (Tor Vergata University, Rome, Italy), Chair, and Prof. Marco Orlandi (Biococca University, Milan, Italy), Co-Chair. Prof. Crestini also is Editor for the conference collection issue to be published in *BioResources.*

REFERENCES CITED

Adler, E., Brunow, G., and Lundquist, K. (1987). "Investigation of the acid-catalyzed alkylation of lignins by means of NMR spectroscopic methods," *Holzforschung* 41(4), 199-207.

Bledzki, A. K., Reihmane, S., and Gassan, J. (1998). "Thermoplastics reinforced with wood fillers: a literature review," *Polymer-Plastics Technology and Engineering* 37(4), 451-468, and references therein.

Bolzacchini, E., Canevali, C., Morazzoni, F., Orlandi, M., Rindone, B., and Scotti, R. (1997). "Spectromagnetic investigation of the active species in the oxidation of propenoidic phenols catalysed by [*N*,*N'*-bis(salicylidene)-ethane-1,2-diaminato]-cobalt(II)," *J. Chem. Soc. Dalton Transactions* 4695-4699.

Buchert, J., Grönqvist, S., Mikkonen, H., Oksanen, T., Peltonen, S., Suurnäkki, A., and Viikari, L. (2005). "Process for producing a fibrous product," *European Pat. 2005*, WO2005061790.

Canevali, C., Orlandi, M., Pardi, L., Rindone, B., Scotti, R., Sipila, J., and Morazzoni, F. (2002). "Oxidative degradation of monomeric and dimeric phenylpropanoids: reactivity and mechanistic investigation," *J. Chem. Soc. Dalton Transactions* 15, 3007-3014.

Canevali, C., Orlandi, M., Zoia, L., Scotti, R., Toppa, E.-L., Sibila, J., Agnoli, F., and Morazzoni, F. (2005). "Radicalization of lignocellulosic fibers, related structural and morphological changes," *Biomacromolecules* 6(3), 1592-1601.

Chandra, R. P., Lehtonen, L. K., and Ragauskas, A. J. (2004). "Modification of high lignin content kraft pulps with laccase to improve paper strength properties. 1. Laccase treatment in the presence of gallic acid," *Biotechnol Prog* 20, 255–261.

Cyr, N. and Ritchie, G. S. (1989). *Lignin Properties and Materials,* W. G. Glasser, S.Sarkanen eds.; American Chemical Society 28, 372-381.

Dence, C. W. (1992). *Methods in Lignin Chemistry*, Y. Lin, C. W. Dence, eds.; Springer-Verlag, Berlin, 33.

Drumond, M., Aoyama, M., Chen, C. L., and Robert, D. (1989). "Substituent effects on carbon-13 chemical shifts of aromatic carbons in biphenyl type lignin model compounds," *J. Wood Chem. Technol*. 9(4), 421-441.

Faix, O., Argyropoulos, D. S., Robert, D., and Neirinck, V. (1994). "Determination of hydroxyl groups in lignins evaluation of 1H-, 13C-, 31P-NMR, FTIR and wet chemical methods," *Holzforschung* 48, 387-394.

Felby, C., Pedersen, L. S., and Nielsen, B. R. (1997a). "Enhanced auto-adhesion of wood fibers using phenol oxidases," *Holzforschung* 51(3), 281-286.

Felby, C., Nielsen, B. R., Olesen, P. O., and Skibsted, L. H. (1997b). "Identification and quantification of radical reaction intermediates by electron spin resonance spectrometry of laccase-catalyzed oxidation of wood fibers from beech (Fagus sylvatica)," *Appl. Microbiol. Biotechnol*. 48(4), 459-464.

Ferm, R., Kringstad, K. P., and Cowling, E. B. (1972). "Formation of free radicals in milled wood lignin and syringaldehyde by phenol-oxidizing enzymes," *Sven. Papperstidn*. 14, 859-865.

Gellerstedt, G., Pranda, J., and Lindfors, E.-L. (1994). "Structural and molecular properties of residual birch kraft lignins," *J. Wood Chem. Technol.* 14(4), 467-482.

Girardin, M., and Metche, M. (1983). "Rapid micro determination of alkoxyl groups by gas chromatography. Application to lignin," *J. Chromatography* 264(1), 155-158.

Himmel, M. E., Tatsumoto, K., Oh, K. K., Grohmann, K., Johnson, D. K., and Li Chum, H. (1989). *Lignin properties and materials,* W. G. Glasser, S. Sarkanen ed. American Chemical Society, chapter 6, 82.

Hon, D. N. S. (1992). *Methods in Lignin Chemistry*, Y. Lin, C. W. Dence, ed. Springer-Verlag, Berlin, 274.

Kilpelainen, I., Sipila, J., Brunow, G., Lundquist, K., and Ede, R. M. (1994). "Application of two-dimensional NMR spectroscopy to wood lignin structure determination and identification of some minor structural units of hard- and softwood lignins," *J. Agr. Food Chem.* 42(12), 2790-2794.

Landucci, L. L. (1985). "Quantitative carbon-13 NMR characterization of lignin 1. A methodology for high precision," *Holzforschung* 39(6), 355-359.

Lund, M., Eriksson, M., and Felby, C. (2003). "Reactivity of a fungal laccase towards lignin in softwood kraft pulp," *Holzforschung* 57, 21-26.

Lund, M., and Felby, C. (2001). "Wet-strength improvement of unbleached kraft pulp through laccase-catalyzed oxidation," *Enzyme Microb. Technol.* 28(9-10), 760-765.

Ralph, J. (1996). "An unusual lignin from Kenaf," *J. Natural. Prod*., 59(4), 341-342.

Robert, D., and Brunow, G. (1984). "Quantitative estimation of hydroxyl groups in milled wood lignin from spruce and in a dehydrogenation polymer from coniferyl alcohol using carbon-13 NMR spectroscopy," *Holzforschung* 38(2), 85-90.

Sipila, J. (2002). *Proceedings of 7th European Workshop of Lignocellulosic and Pulp*, Turku 26-29 August, 67-70.

Sippola, V. O., and Krause, A. O. I. (2003). "Oxidation activity and stability of homogeneous cobalt-sulphosalen catalyst. Studies with a phenolic and a non-phenolic lignin model compound in aqueous alkaline medium." *Journal of Molecular Catalysis A: Chemical* 194(1-2), 89-97.

Article submitted: Sept. 18, 2007; First round of peer review completed: Nov. 1, 2007; Revised article received and approved: Nov. 26, 2007; Published, Nov. 27, 2007.

HYDROPHOBICALLY MODIFIED PECTATES AS NOVEL FUNCTIONAL POLYMERS IN FOOD AND NON-FOOD APPLICATIONS

Zdenka Hromádková,[a] Anna Malovíková,[a*] Štefan Mozeš,[b] Iva Sroková,[c] and Anna Ebringerová[a]

Butyl and hexyl amides of pectate with various amidation degrees were prepared from citrus pectin by means of alkylamidation of methyl-esterified pectins, followed by the total alkaline pectin methyl esters hydrolysis. These water soluble derivatives were characterized chemically as well as by elementary analysis and FT-IR spectroscopy. All prepared pectate amides exhibited the excellent emulsifying efficiency, and pectate hexyl amide also the ability to form stable foam. As the results of the study on the effect of pectin with DE 66% on the function of small intestine in pectin fed rats, the increase of specific activity of alkaline phosphatase, maltase, and aminopeptidase and the decrease of food utilization was demonstrated. The pectin derivatives might serve as emulsifiers and foaming additives in food production and other areas as well as nutraceuticals for obesity treatment.

Keywords: Pectin, Modification, Pectate alkylamides, Surface activity, Intestine enzymes, Obesity

*Contact information: a: Institute of Chemistry, Center for Glycomics, Slovak Academy of Sciences, 845 38 Bratislava, Slovak Republic; b: Institute of Animal Physiology, Slovak Academy of Sciences, 040 01 Košice, Slovak Republic; c: Department of Chemistry and Technology of Rubber and Textile, Faculy of Industrial Technologies, Trenčín University of Alexander Dubček, 020 32 Púchov, Slovak Republic; * Corresponding author : chemmalo@savba.sk*

INTRODUCTION

Pectin is one of the commercial polysaccharides produced from agricultural by-products- citrus peels and apple pomace. These pectins are complex acidic polysaccharides with a linear backbone of (1-4)-α-D-galacturonic acid units, which are partially methylesterified and bear as side chains neutral sugars of the arabinogalactan type (Thakur et al. 1997). There is a continuing interest in exploitation of the pectin component from other plant residues. The expanding uses of pectin within the food and pharmaceutical industries increases the demand for pectins and pectin-rich plant sources. Next to the citrus peels and apple pomace, various other agricultural by-products are available, such as sugar beet pulp (Michel et al. 1985), pumpkin peel (Jun et al. 2006), sunflower heads, grape and olive pomaces, etc. (Thakur et al. 1997).

Pectin is widely used in the food industry as a hydrocolloid additive with gelling, thickening and stabilizing properties, as well as recognized as a dietary fibre playing a significant role in reducing the risks of the high life style-related diseases - cardiovascular and gastrointestinal ones, obesity, diabetes, etc. (Prosky 2001). Among the many areas in obesity research, diet supplementation with pectin suggested as a fat-replacer, decreased

digestion and absorption of nutrients (Dvir et al. 2000; Drochner et al. 2004) and function of the small intestine (Chun et al. 1989). In relation to the prevention and treatment of obesity, there is a lack of knowledge on the effect of the structural features of pectin (such as the degree of methylesterification) as well as of partial hydrophobic modification, which are assumed to contribute to intermolecular interactions with the intestinal mucous membranes.

Hydrophobically modified pectins, such as alkyl esters of pectin and pectic acid (Klavons and Bennet 1995; Pappas et al. 2004) have been suggested as emulsifiers in cosmetic and pharmaceutical cream formulations, and as stabilizers or beverage clouding agents. Pectin amides (Reitsma et al. 1986; Anger and Dongowski 1988; Sinitsya et al. 2000) were reported to possess good gelling properties important in the low sugar diets, and useful as sorbents (Sinitsya et al. 2004). These pectin amides contain both methyl ester and amide groups. To our best knowledge, pectin amides without methyl ester groups (pectate amides) have not yet been studied.

The aims of the present paper were

- (i) to prepare a novel series of pectate derivatives with some carboxyl groups transformed into C_4- and C_6-alkylamides using the commercial citrus pectin as model pectin and characterize their structural and surface active properties, and
- (ii) to study the changes in the specific activity 'in vivo' of some enzymes of the small intestine and their possible role in the mechanisms that influence the rate of nutrient absorption under high fat diet feeding conditions using the model citrus pectinate.

EXPERIMENTAL

Materials

Commercial citrus pectin with degree of methylesterification DE = 66% (PE66) was from Danisco, Smiřice (Czech Republic). It contains 85% galacturonic acid and 15 % neutral sugars. The highly esterified pectin with DE 93% (PE93) was prepared from the commercial pectin at the Institute of Chemistry, Slovak Academy of Sciences (Bratislava, Slovakia) by esterification in acidic methanol. Both pectin preparations were used for the synthesis of amidated derivatives and physiological studies. The commercial citrus pectin amide (PE-NH2) was kindly donated by Danisco (Smiřice, Czech Republic). The butyl and hexyl amines were from Merck (Germany). Alkaline phosphatase (AP) and aminopeptidase (AMP) were from Sigma-Aldrich (USA), and maltase was from Glycosynth (UK). High-fat (HF) diet was from Research Diet (USA).

Analytical Methods

DE was determined by precipitation of the insoluble copper pectates and pectinates (Tibenský et al. 1963). The degree of amidation (DA) was calculated using the following equation (Sinitsya et al. 2000):

$$\% \text{ DA} = \%N / \%C \times [6 + DE/100 + (K-1) \times \%N / 14] \times 100, \quad (1)$$

where the % of carbon (C) and nitrogen (N) were determined by elementary analysis using analyser model 240 (Perkin-Elmer). Fourier-transform infrared (FT-IR) spectra of the samples (2 mg/200 mg KBr) were obtained on the NICOLET Magna 750 spectrometer with DTGS detector and OMNIC 3.2 software using 128 scans at a resolution of 4 cm^{-1}.

Synthesis of Pectate Alkyl Amides

The synthesis was carried out in two steps. In the first step the reaction was carried out with primary alkyl amines (butyl, hexyl) in a heterogeneous system using methanol at 5°C for 10–20 h according to Sinitsya et al. (2000). In a typical experiment, the pectin (15 g) was suspended in 150 ml dry methanol and hexylamine (90 ml) was added under stirring. The reaction proceeded at 5°C for 20 h. Then the products were washed with chloroform to remove the unreacted amine. The wet samples were treated with 0.1 M HCl in ethanol–water mixture (2:1, v/v) to convert carboxylates into their protonated form, washed with neutral ethanol, and air-dried yielding pectinic acid alkylamides. In the second step, these derivatives were further deesterified in alkaline medium in a suspension of 70% ethanol for 12 h, and the obtained pectate alkylamides were recovered by successive washing with ethanol and acetone, and drying on air.

Surface-Activity Testing

The emulsifying efficiency was tested on emulsions of the oil in water (O/W) type as described by Sroková et al. (2003). The emulsion was prepared by mixing a solution (0.05 g of the derivative in 9 ml water) and 1 ml of paraffin oil dyed with SUDAN IV in the laboratory mixer at 20,500 rpm for 1 min. The stability of the emulsion was estimated at three different time intervals after the emulsions had been prepared, i. e. 5 min (h_1), 1h (h_2) and 24h (h_3), and expressed in terms of the height (mm) of the oil and cream layers formed on the surface of the emulsion. The surface tension of aqueous polysaccharide solution in the concentration range 0.015-2.5 $g.l^{-1}$ was determined at 25°C using the Du Nouy ring apparatus.

Enzyme Activity testing

Male Sprague-Dawley rats (30 day old) fed with high fat/high energy (HF) diet (4.04 kcal/g; 14.5% energy as protein, 30% as fat and 55.5% as carbohydrate) were divided into three groups: 1. control group (C), which was allowed free access to HF diet, 2. pectin group (P) receiving the same diet containing 15% (w/w) of the citrus pectin (PE66), 3. PF group, pair-fed to food intake of pectin fed group for 10 days. The activities of alkaline phosphatase (AP), maltase and aminopeptidase (AMP) were tested using a modified simultaneous azo-coupling method (Lojda et al. 1979, Nachlas et al.1960). Enzyme activity in a cryostat tissue sections (8 μm) was histochemically (cytophotometrically) analysed with a Vickers M85a microdensitometer. The measurements were performed using a x 40 objective, an effective scanning area of 28.3 μm^2 and a scanning spot 0.5 μm in at least 30 brush border areas along the villus length in five sections of the jejunum. The integrated absorbance of enzyme activity was calculated as the absorbance values recorded by the instrument in min/mm^{-3} brush border ± SE and these mean values were referred to one animal.

The measurements were performed using a x 40 objective, an effective scanning area of 28.3 μm^2 and a scanning spot 0.5 μm. The integrated absorbance of enzyme activity along the villus length of the jejunum was calculated as the absorbance values recorded by the instrument in min/mm^{-3} brush border ± SE.

RESULTS AND DISCUSSION

The alkylamidation of the model pectins was performed in two-steps by:
(i) introduction of alkylamide groups yielding the intermediate derivative of pectinic acid alkylamide and (ii) removal of the methoxyl groups yielding the pectate alkyl amides. All derivatives were water-soluble. The derivatives were characterized by FT-IR spectra (Fig. 1a). The vibrations of the Amide I and Amide II at 1655 cm^{-1} and 1550 cm^{-1}, respectively, as well as the C=O streching vibration of the ester and carboxylate groups at 1751 cm^{-1} and 1600 cm^{-1}, respectively, were differentiated using peak-fitting (Fig. 1b). The chemically determined degree of esterification (DE) and degree of amidation (DA) of both the intermediate and final products are sunmmarized in Table 1. As seen in Table 1, the chemical modification of pectins was accompanied by depolymerization, indicated by the decrease of the intrinsic viscosity.

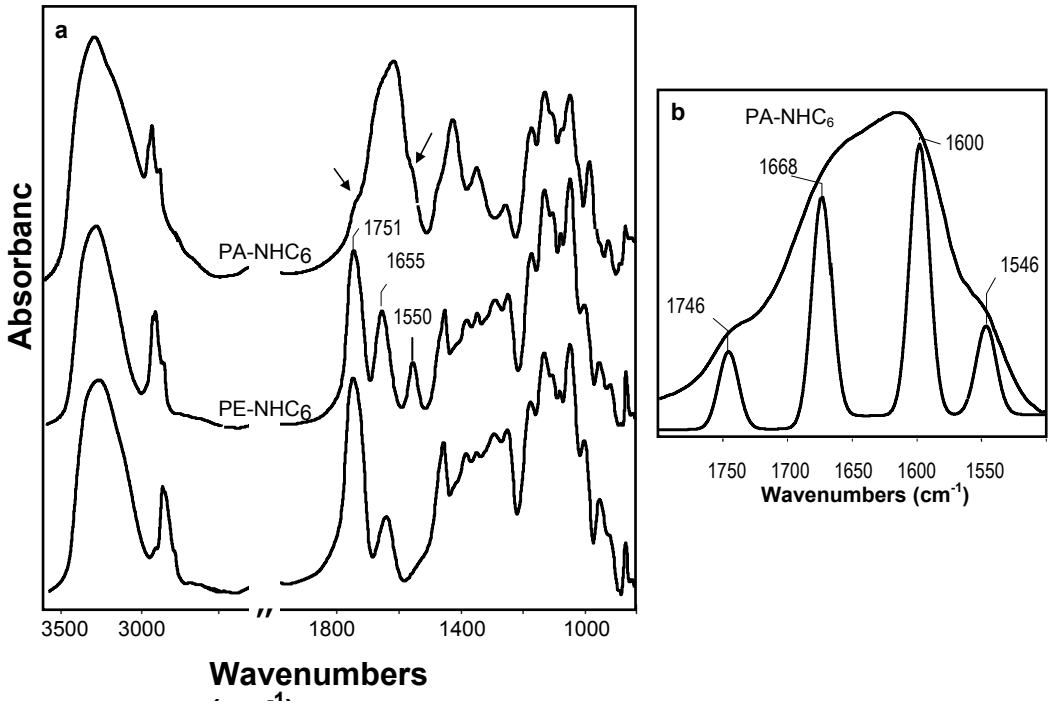

Fig. 1. FT-IR spectra in KBr of (a) the starting pectin (PE93), pectinic acid hexylamide (PE-NH_6) and pectate hexylamide (PA-NHC_6), and (b) the partial spectrum of PA-NHC_6 obtained by peak-fitting. The arrows indicate the Amide I and Amide II bands.

The surface activity of the original pectins, their butyl and hexyl amide intermediates and final pectate amides were tested for surface tension and emulsifying efficiency. All tested samples gave stable oil-in water emulsions.

The substitution of the methyl ester groups by alkyl amide groups resulted in very pronounced foaming, depending on the alkyl length and DA. With the hexyl derivatives the foam was stable after 24 h. Despite these properties, the surface-activity depressing effect of the derivatives was very low (69.7-59.8 $mN.m^{-1}$). Similar effects were observed with polymeric surfactants prepared from other polysaccharides such as from hydroxyethylcellulose (Sroková et al. 2003).

Table 1. Analytical Data and Surface Active Properties of Pectins and their Derivatives

Sample	DE	DA	[η]	Oil/Cream layers[a] (mm/mm)			γ_{min}	c.m.c.
	%	%	($ml.g^{-1}$)	5 min	1h	24 h	mN.m-1	$g.l^{-1}$
Original pectin								
PE66	66	0	434	0/0	0/0	0/12	nd	nd
PE93	93	0	132	0/8	0/11	0/11	nd	nd
Pectinate amide and alkyl amides								
PE-NH_2	31	24	395	0/0*	0/0*	0/10*	59.8	1.08
PE-NHC4	85	13	92	0/0*	0/8*	0/11	69.7	1.37
PE-NHC6	nd	nd	176	0/0*	0/0*	0/7*	62.7	0.62
Pectate amide and alkyl amides								
PA-NH_2	0	23	229	0/0	0/4	0/9	68.8	1.25
PA-NHC4	0	15	42	0/2	0/7	0/8	no	no
PA-NHC6	3	30	85	0/0*	0/10*	0/10	63.4	0.31
Tween 20				0/0	0/0	0/4		

[a]Oil/water emulsion: Height of oil and cream layers formed on the surface of the emulsion after 5 min, 1 h and 24 h; * Foaming; Tween 20, commercial synthetic emulsifier.

As a preliminary study of the effect of pectin and their derivatives on the function of the small intestine, the citrus pectin (PE66) was tested for changes in the activity of the small intestine enzymes AP, maltase and AMP in pectin fed rats. As illustrated in Table 2, the activity of these enzymes in the pectin group animals (P) significantly raised by 18%, 25%, and 23% respectively, in comparison with values of the control animals (C). These results are in accord with the reports about the increased activities of intestinal brush border bound enzymes using diet supplemented with pectin (Chun et al. 1989; Farness and Schneeman 1982).

The observed functional changes were also associated with significantly decreased food intake, food efficiency, as well as with significantly lowered epididymal plus retroperitoneal fat pad weight. These somatic changes were also associated with the alteration of the weight gain parameters (Control 48.0±2.1, Pectin 22.6±1.5*, PF±29.1*). Moreover, in the pectin fed animals (PF) as compared to C animals, the reduced intake of high fat (HF) diet did not change the intestinal enzyme and body fat parameters. This indicates that up-regulation of enzyme activities in P group is rather a consequence of specific effect of pectin than the decrease of luminal nutrition. Further studies with other pectins and pectin amide derivatives are in progress. The obtained results about the effect of pectin on the function of the small intestine can expand the knowledge on the

participation of the small intestine in the mechanisms that might play a key role on influence development of obesity and associated feeding and body fat disturbances.

Table 2. Effect of Citrus Pectin (PE66) on the Function of Small Intestine in Pectin-Fed Rats

Group	AP	Maltase	AMP	Body fat %	Food intake g/day	FE
Control	13.4±0.6	14.2±0.5	14.3±0.5	0.73±0.07	12.3±0.5	0.39±0.01
Pectin	15.8±0.2*	17.8±0.9*	17.6±0.9*	0.27±0.03*	9.6±0.8*	0.24±0.02*
PF	13.1±0.1#	14.6±0.4#	13.7±0.5#	0.64±0.03#	10.1±0.4*	0.30±0.01*#

Values are means ± SE (n = 8 animals/groups); Enzyme activity is given as a density values in jejunal enterocytes at wavelength of 520 nm; AP (Alkaline phosphatase), AMP (Aminopeptidase) and Maltase are intestinal enzymes; Body fat (%) represents epididymal plus retroperitoneal fat pads weight; FE (food efficiency) is given as the weight gain/food intake; * significantly different from C group; # significant differences between P and PF groups at $P<0.05$ by Tukey's test after ANOVA.

CONCLUSIONS

1. The results suggested that the novel butyl and hexyl amide pectates with DA ranging between 15-30% represent polymeric surfactants with excellent emulsifying efficiency, and in the case of the hexyl derivatives the ability to produce stable foams.
2. The derivatives are potential polysaccharide-based biodegradable surfactants useful in various technical applications and industrial processes.
3. The results of the effect of the pectin on the energy homeostasis of rats suggested that the enhanced activity of enzymes and decreased food utilization observed in pectin-fed rats might play an important role in prevention the development of obesity on high fat diet.

ACKNOWLEDGEMENTS

This work was financially supported by the Slovak Grant Agency VEGA (grant No. 2/6131/26 and 2/5141/25) and the agency APPV (project COST-0036-06).

This contribution was an original presentation at the *ITALIC 4 Science & Technology of Biomass: Advances and Challenges* Conference that was held in Rome, Italy (May 8-10, 2007) and sponsored by Tor Vergata University. The authors gratefully acknowledge the efforts of the Conference Organizers, Prof. Claudia Crestini (Tor Vergata University, Rome, Italy), Chair, and Prof. Marco Orlandi (Biococca University, Milan, Italy), Co-Chair. Prof. Crestini also is Editor for the conference collection issue to be published in *BioResources.*

REFERENCES CITED

Anger, H., and Dongowski, G. (1988). "Amidated pectins–characterization and enzymatic degradation," *Food Hydroclloids* 2(5), 371-379.

Chun, W., Bamba ,T., and Hosoda, S. (1989). "Effect of pectin a soluble dietary fiber on functional and morphological parameters of the small intestine in rats," *Digestion* 42(1), 22-29.

Drochner, W., Kerler, A., and Zacharias, B. (2004). "Pectin in pig nutrition, a comparative review," *J. Anim. Physiol. Anim. Nut.* 88(11-12), 367-380.

Dvir, I., Chayoth, R., Sod-Moriah, U., Shany, S., Nyska, A., Stark, A. H., Madar, Z., and Arad, S. M. (2000). "Soluble polysaccharide and biomass of red microalga *Porfyridium sp.* alter intestinal morphology and reduce serum cholesterol in rats," *Br. J. Nutr.* 84(4), 469-476.

Farness, P. L., and Schneeman, B. O. (1982). "Effect of dietary cellulose, pectin and oat bran on the small intestine in the rat," *J. Nutr.* 112(7), 1315-1319.

Jun, H. I., Lee, Ch.-H., Song, G.-S., and Kim, Z.-S. (2006). "Characterization of the pectic polysaccharides from pumpkin peel," *LWT-Food Sci. Technol.* 39(5), 554-561.

Klavons, J. A., and Bennet, R. D. (1995). "Preparation of alkyl esters of pectin and pectic acid," *J. Food Sci*. 60(3), 513-515.

Lojda, Z., Gossrau, R. and Schibler, T. H. (1979). "A laboratory manual," *Enzyme Histochemistry,* Springer-Verlag, Berlin.

Michel, F., Thibault, J. F., Mercier, C., Heitz, F., and Pouillaude, F. (1985). "Extraction and characterization of pectins from sugar beet pulp," *J. Food Sci.* 50(5), 1499-1500.

Nachlas, M. M., Monis, B., Rosenblatt, M. D., and Seligan, A. M. (1960). "Improvement in the histochemical localization of leucine aminopeptidase with a new substrate, L-leucyl-4-methoxy-2-napthamide," *J. Biophys. Biochem. Cytol*. 7, 261-264.

Pappas, CH. S., Malovíková, A., Hromádková, Z., Tarantilis, P. A., Ebringerová, A., and Polissiou, M. G. (2004). "Determination of the degree of esterification of pectinates with decyl and benzyl ester groups by diffuse reflectance infrared Fourier transform spectroscopy (DRIFTS) and curve-fitting deconvolution method," *Carbohydr. Polym.* 56(4), 465-469.

Prosky, L. (2001). "*Advanced Dietary Fiber Technology*," Bleackwell Science, Oxford 2001.

Reitsma, J. C. E., Thibault, J. F., and Pilnik, W. (1986). "Properties of amidated pectins. I. Preparation and characterization of amidated pectins and amidated pectic acids," *Food Hydrocolloids* 1(2), 121-127.

Sasinková, V., Hromádková, Z., Malovíková, A., Sroková, I., and Ebringerová, A. (2005**). "**Hydrophobically modified citrus pectin with pendant alkyl amine groups**,"** *Book of Contribution, 4th Conference Structure and Stability of Biomacromolecules SSB 2005,* Košice, Slovakia, p. 95.

Sinitsya, A., Čopíková, J., Prutyanov, V., Skoblya, S., and Machovič, V. (2000). "Amidation of highly methoxylated citrus pectin with primary amines,"

Carbohydr. Polym. 42(4), 359-368.
Sinitsya, A., Čopíková, J., Marounek, M., Mlčochová, P., Sihelníková, L., Skoblya, S., Havlátová, H., Matějka, P., Maryka, M., and Machovič, V. (2004). "*N*-octadecylpectinamide, a hydrophobic sorbent based on modification of highly methoxylated citrus pectin," *Carbohydr. Polym*. 56(2), 169-176.
Sroková, I., Miníková, S., Ebringerová, A., and Sasinková, V. (2003). "2-Hydroxyethyl)cellulose-based nonionic biosurfactants," *Tenside Surf. Det.* 40(1), 73-76.
Thakur, B. R., Singh, R. K., and Handa, A. K. (1997). "Chemistry and uses of pectin," *Crit. Rev. Food Sci. Nutr.* 37(1), 47-73.
Tibenský, V., Rosík, J. and Zitko, V. (1963). "Zur Bestimmung des Veresterungsgrades von Pektin," *Nahrung* 7(4), 321-325.

Article submission received: Sept. 19, 2007; First round of peer-review completed: Nov. 27, 2007; Revision received and accepted: Dec. 6, 2007; Published: Dec. 8, 2007

HUMIC ACID-LIKE MATTER ISOLATED FROM GREEN URBAN WASTES. PART I: STRUCTURE AND SURFACTANT PROPERTIES

Enzo Montoneri,[1*] Vittorio Boffa,[1] PierLuigi Quagliotto,[1] Raniero Mendichi,[2] Michele R. Chierotti,[3] Roberto Gobetto,[3] and Claudio Medana[4]

A humic acid-like substance (cHAL2) isolated from urban green wastes before composting was compared to a humic acid-like substance (cHAL) isolated from a mix of urban organic humid waste fraction and green residues composted for 15 days. cHAL2 was found to contain more aliphatic and O-alkyl C atoms relative to aromatic, phenol, and carboxyl C atoms, and to yield higher critical micellar concentration (cmc = 0.97 g L^{-1}) and surface tension at the cmc (γcmc = 37.8 mN/m) in water than cHAL (cmc = 0.40 g L^{-1}; γcmc = 36.1 mN/m). The results point out that biomass wastes may be an interesting source of biosurfactants with diversified properties that depend on the nature of waste and on its process of treatment.

Keywords: Urban refuse; Compost; Biosurfactants; Humic acids; Biomass.

*Contact information: [1]Dipartimento di Chimica Generale ed Organica Applicata, Università di Torino, C. M. D'Azeglio 48, 10125 Torino, Italy; [2]Istituto per lo Studio delle Macromolecole (CNR), Via E. Bassini 15, I-20133 Milano, Italy; [3]Dipartimento di Chimica I.F.M., Università di Torino, Via P. Giuria 7, 10125 Torino, Italy; [4]Dipartimento di Chimica Analitica, Università di Torino, Via Pietro Giuria 5, 10125 Torino, Italy; *Corresponding author: enzo.montoneri@unito.it*

INTRODUCTION

Separate collection of urban food and green wastes and their compost products are interesting low entropy sources of organic C. They are available from confined spaces, and may have relatively low water (35-55 %) and high organic matter (26-50 %) contents (Quagliotto 2006; Ozores-Hampton and Obreza 2007). Recycling of the organic matter of these wastes for further uses is a worthwhile scope to be pursued for economic and environmental reasons. Composting is carried out nowadays in public and private facilities throughout the world (Kraft 2006; Newman 2006; Ozores-Hampton and Obreza 2007; Stoffella 1997) at a processing tipping fee of about 70 €/ton, while the compost product is proposed as fertilizer at a current market value which is not above 15 €/ton. Therefore, composting urban humid and vegetable residues has a net cost of about 55 €/ton. Very recently we have shown that compost is a rich source of biosurfactants and suggested that these materials may have a range of potential applications in the chemical industry. Indeed a humic acid-like compound isolated from compost was found to have quite remarkable surfactant properties (Quagliotto 2006) and good performance as a chemical auxiliary for dyeing nylon 6 (Savarino 2007). For the sake of simplicity, we

refer to this compound as cHAL. Composting, however, yields a wide range of different products, depending on the compost wastes mix and the composting time. As these compounds might in principle offer a range of properties from which to choose those tailored for specific needs, we wish to report herewith the structure and surfactant properties of a new compost isolated humic acid-like substance (here and after named cHAL2). Compared to cHAL, isolated from a mix of urban organic humid waste fraction and green residues composted for 15 days, cHAL2 was isolated from green urban wastes only before composting. Our long range purpose is to build a data inventory which at some point will make it possible not only to understand how the parameters characterizing the waste nature and the composting process influence the structure and surfactant properties of the isolated humic-like substances, but also to assess how much the source and structural difference of these substances affect their performance as auxiliaries for chemical technological uses.

EXPERIMENTAL

All reagents were Aldrich products, unless otherwise indicated. Ground urban green wastes, collected from the Amiat municipal plant in Torino, Italy were extracted according to a known procedure (Quagliotto 2006) to yield, in 12 % w/w yield relative to the starting dry waste, the humic acid-like material (cHAL2) investigated in this work. This material was found to contain 7.47 % water, 91.60 % volatile solids and 0.93 % ash by the weight losses measured after heating first at 105 and then at 800 °C. Further characterization for cHAL2 was performed by elemental analysis, solid state ^{13}C and solution ^{1}H NMR spectroscopy, IR spectroscopy, and surface tension measurements as previously reported (Quagliotto 2006). The determination of free phenol and carboxylic acid groups (Table 1) was accomplished by potentiometric titration according to a previous procedure (Brunelot 1989). Under our experimental conditions, deionized water was boiled under nitrogen atmosphere to remove dissolved CO_2. This water was used to make the required sample and reagents solutions. The cHAL2 sample was dissolved at 1.87 g/L concentration in 0.015 N NaOH. The total alkali content in the solution was in excess relative to the total cHAL2 carboxyl and phenoxide content (Table 1) determined by ^{13}C NMR spectroscopy. This solution with pH about 12 was titrated with standardized 0.01 N aqueous HCl. Similar titration was performed on a blank solution containing the same amount of alkali as the above sample solution, but no cHAL2. The titrations were performed at 25 °C using an automatic Cryson Compact Titrator with a resolution of 1 µl of titrant in a thermostated glass cell under nitrogen blanketing to prevent dissolution of atmospheric carbon dioxide in the sample.

Under these experimental conditions, it was possible to obtain a potentiometric curve of satisfactory quality (Fig. 1). The elaboration of the experimental data (pH versus titrant volume in Fig. 1a) obtained under this condition is based on the linearization functions proposed by Gran (1952). According to the above method, from the linearized data plotted in Fig. 1b it was possible to extrapolate 3 equivalence points. Two of these points were obtained from the sample (cHAL2) titration curve and correspond to the added titrant volumes Va and Vb. The third equivalence point, corresponding to the

added titrant volume Vc, indicates the endpoint of the titration of the blank alkali solution. This solution contained the same amount of added NaOH as the above titrated cHAL2 solution, but did not contain any cHAL2. In addition to these equivalence points, other two points, corresponding to the added titrant volumes Ve_1 and Ve_2, were extrapolated from the first derivative of the cHAL2 titration curve in Fig. 1a. Based on the pH values measured at each of the above titrant volumes, the following assignments are given: i.e., Vb is considered the HCl volume necessary to titrate the excess NaOH over the sample total acidity, Vb-Ve_1 is the HCl volume necessary to convert all ArONa groups to ArOH, and Ve_2-Ve_1, Va – Ve_2 and Vc-Va correspond to the volumes of HCl necessary to convert the sodium salts of carboxylic acids with increasing acidity strength to their free acid –COOH forms.

Table 1. Data[a] Found for cHAL[b], cHAL2[c] and Peat Humic acid (PHA)[d,e]

	C w/w %	Empirical Formula				
		C	H	N	O	S
cHAL	59.9[b]	10	13.4	0.86	3.4	0.036
cHAL2	57.9[c]	10	12.6	0.63	3.0	0.018
PHA	50.4-58.8[d,e]	10	7.3-12.7	0.25-0.52	4.6-5.8	0.052

	pH	COX[f] meq/g	COOH meq/g	ArOY[f] meq/g	ArOH meq/g	MW
cHAL	4.00	5.71	1.10[g]	3.38	1.90[g]	15610
cHAL2	3.96	3.56	2.91[g]	2.46	0.87[g]	217630[h]
PHA			2.76[e]		3.28[e]	17000[e]

[a]C content (w/w %) in ash free dry matter, elements atoms in empirical formula, pH of a water suspension (12 mg/30 mL) containing 0.01 N NaCl, free carboxylic (COOH) and phenol (ArOH) groups, weight(MW) and number-(MN) averaged molecular weights defined as previously reported (*22*).
[b]Isolated in previous work (Quagliotto 2006).
[c]Isolated in this work..
[d]Peat (Montoneri 2003).
[e]Peat (Terashima 2004).
[f]Total carboxyl (X = H or N) or phenoxide (Y = H, R, Ar) contents = A/(1201.1 B), A = % band relative area from column 8 (carboxyl) or column 7 (phenoxide) in Table 2; B = 10^{-2} C w/w % from Table 1.
[g]By potentiometric titration.
[h]Data obtained in this work by SEC-MALS.

Dynamic light scattering (DLS) measurements were obtained with a ZetaSizer® (Malvern, UK), which has a detection window included between about 0.6 nm and 5 μm. The measurements were carried at pH 7.0 and 25 C after filtering the cHAL2 sample solution on a cellulose acetate disk (Schleicher & Schuell) with a size cut-off of 0.8 μm. The CONTIN method (Provencher 1976) was used to analyze the DLS data for calculating the hydrodynamic diameter (D_h) of the molecules or aggregates in solution.

Electrospray ionization measurements (ESI) were obtained using a LTQ Orbitrap high mass (M) resolving power (R = M/ΔM) spectrometer (Thermo, Rodano, Italy), with electrospray interface and ion trap as mass analyzer. The flow injection effluent was delivered into the ion source using nitrogen as sheath and auxiliary gas (flow rate 10 μL/min). The source voltage was set at 4.0 kV in the negative ion mode. The heated capillary was maintained at 270°C. The tuning parameters adopted for the ESI source were the following: source current 100 μA, capillary voltage -9 V, tube lens -120 V. Mass spectra were collected in full scan negative mode in different ranges between 200 and 1500 mass to charge (m/z) ratio.

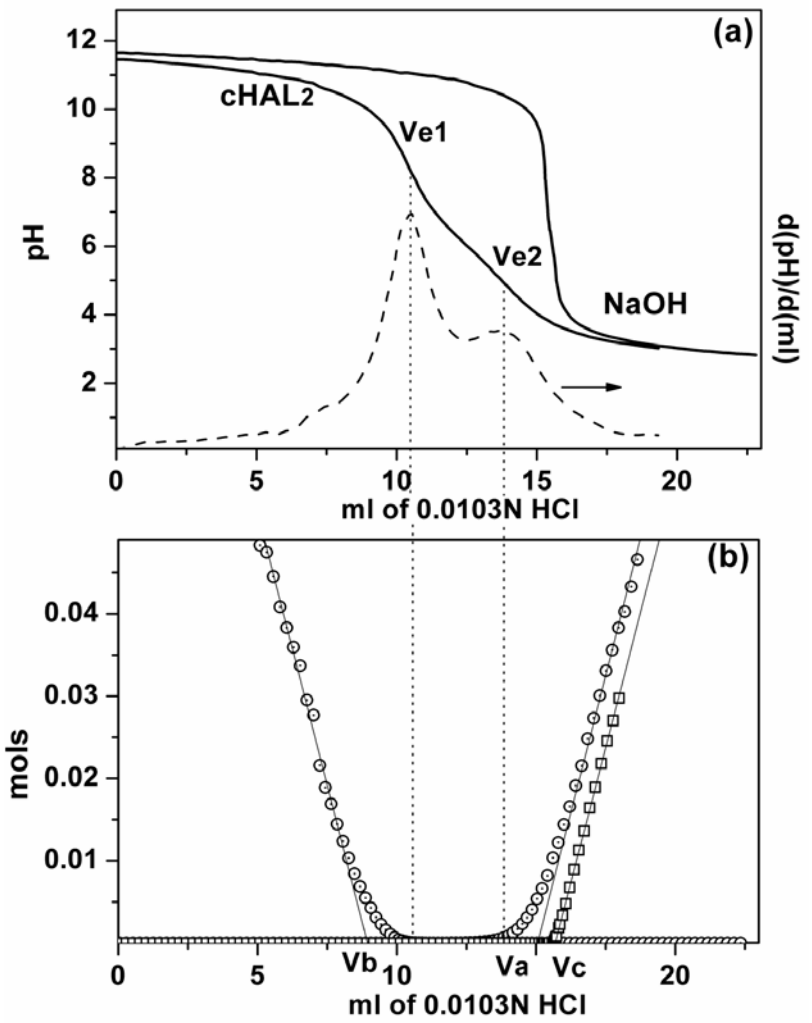

Fig. 1. Potentiometric titration of cHAL2. (a) Titration of 10 ml of a 0.0156 N NaOH solution dissolved in 30 ml of water and back-titration of 18.7 mg of cHAL2 dissolved in 10 ml of aqueous NaOH 0.0156 N and diluted in 30 ml of water. The dashed line indicates the first derivative (dpH/dml) of the cHAL2 back-titration. (b) Linearization of the NaOH titration curve (□) and of the cHAL2 back-titration curve (○) according to the Gran method (Gran 1952).

Molecular investigation was performed also through fractionation and characterization by a multi-angle laser light scattering (MALS) detector on-line to a size exclusion chromatography (SEC) system. The SEC-MALS system consisted of an Alliance 2690 separation module, a 2414 differential refractometer (DRI) from Waters (Milford, MA, USA), and a MALS Dawn DSP-F photometer from Wyatt (Santa Barbara, CA, USA). This multi-detector SEC-MALS system was described in detail previously (Mendichi 2001). The wavelength of the MALS laser was 632.8 nm. The light scattering signal was detected simultaneously at fifteen scattering angles ranging from 14.5° to 151.3°. The calibration constant was calculated using toluene as standard, assuming a Rayleigh factor of $1.406 \cdot 10^{-5}$ cm^{-1}. The angular normalization was performed by measuring the scattering intensity of a concentrated solution of BSA globular protein in the mobile phase assumed to act as an isotropic scatterer. The refractive index increment, dn/dc, with respect to the solvent was measured by a KMX-16 differential refractometer from LDC Milton Roy (Riviera Beach, FL, USA). The dn/dc value for cHAL2 was 0.214 mL/g. The humic acid-like substance solubilization procedure and the SEC experimental conditions were quite similar to those previously reported (Kawahigashi 2005)**.** The starting sample solution contained cHAL2 at 1 g L^{-1} concentration in 0.01M K_2HPO_4-0.01M KH_2PO_4 aqueous buffer (pH 7.0) containing 10% methanol. The same solvent was used as SEC mobile phase under the following conditions: single aqueous Shodex OHpak KB805 column from Showa Denko (Tokyo, Japan), 35 °C temperature, 0.8 mL/min flow rate and 100 µL sample injection volume.

RESULTS AND DISCUSSION

To understand compositional and structural difference between materials isolated from composted wastes, one should first consider that composting is an aerobic biodegradation process of refuse biomass, leading to some mineralization of the original organic C and N and to chemical modifications of the remaining organic residue (Genevini 2002). Compared to the starting biomass waste, the composted waste is generally characterized by a lower content of polysaccharides, and by a relatively higher concentration of lignin-like material. Changes also involve chemical identities. Native lignin is modified to lignin-humus. The latter material, although not well defined, is usually characterized by its aliphatic/aromatic C ratio and by its content of carboxylic and phenolic functional groups. The humic acid-like organic fraction is separated (Montoneri 2003a) from the polysaccharide, protein, fats and other humic-like matter by extraction of the starting biomass with alkali and precipitation of the humic acid-like fraction at pH < 1.5. In our case, the humic acid-like material investigated in this work (cHAL2) was isolated from urban green wastes that were sampled right before composting. By comparison, our previously investigated (Quagliotto 2006) humic acid-like material (cHAL) was isolated from a 1:1 v/v mixture of food residues and public parks green wastes that had been composted for 15 days. To evidence the structural features of cHAL2, we like to refer to the above previous cHAL material for which the structure represented in Fig. 2 was proposed, based on the elemental analysis, acid groups

determination, and NMR data. Tables 1-3 report these characterization data for both cHAL and cHAL2.

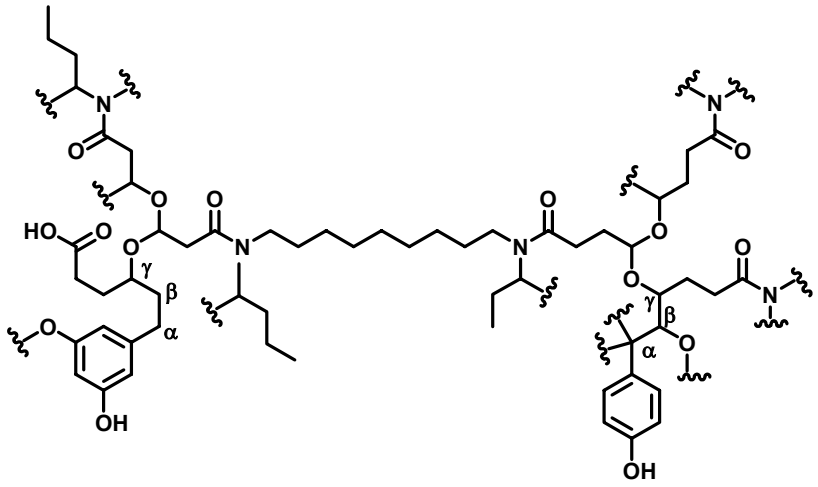

Fig. 2. Proposed molecular fragment for cHAL (Quagliotto 2006). H bonded to C omitted; sinusoidal bold lines indicate other fragments C, O, N atoms.

From Fig. 2 the cHAL structure may be visualized as an elongated hydrophobic portion made by a central 9 C long chain and by peripheral 2-3 C short chain aliphatic amide and di-O alkyl ether groups, to which two polar hydrophilic substituted propylphenol hydrocarbon residues are attached. The data obtained for cHAL2 (Tables 1-3) show that this material, compared to cHAL, is likely to have some significant structural differences: i.e., relative to the composition of the molecular fragment represented in Fig. 2 for cHAL, cHAL2 has 15 short chain aliphatic C, 5 O-alkyl C and 1 di-O-alkyl C more (Table 2). On an eq/g concentration basis, these features are accompanied by a relatively lower content of carboxyl and phenoxide functional groups (Table 1).

One aspect deserving particular attention in the characterization of humic acid-like substances is the determination of acid groups. It may be observed from the data in Table 1 that large fractions of the carboxyl and phenoxide groups consist of free carboxylic acids (-COOH) and phenolic (ArOH) groups. For the determination of these groups we have adopted the method suggested by Brunelot et al. (1989) for the potentiometric titration of humic and fulvic acids. As pointed out in the experimental section, these authors suggest that the potentiometric titration method may also yield the breakdown of carboxylic acids into functional groups with increasing acidity strength. We are convinced that this point would deserve deeper investigation in a specifically dedicated work. Within the more general issue addressed by our work, we are content with reporting the results in Table 1 as phenol (ArOH) and total carboxylic acid (COOH) groups. It may be observed that the values obtained for these groups by the above potentiometric titration method are consistent with the data obtained for total carboxyl

and total phenoxide groups by ^{13}C NMR spectroscopy (Fig. 3), inasmuch as the free acid groups turn out a fraction of the total phenoxide and carboxyl groups.

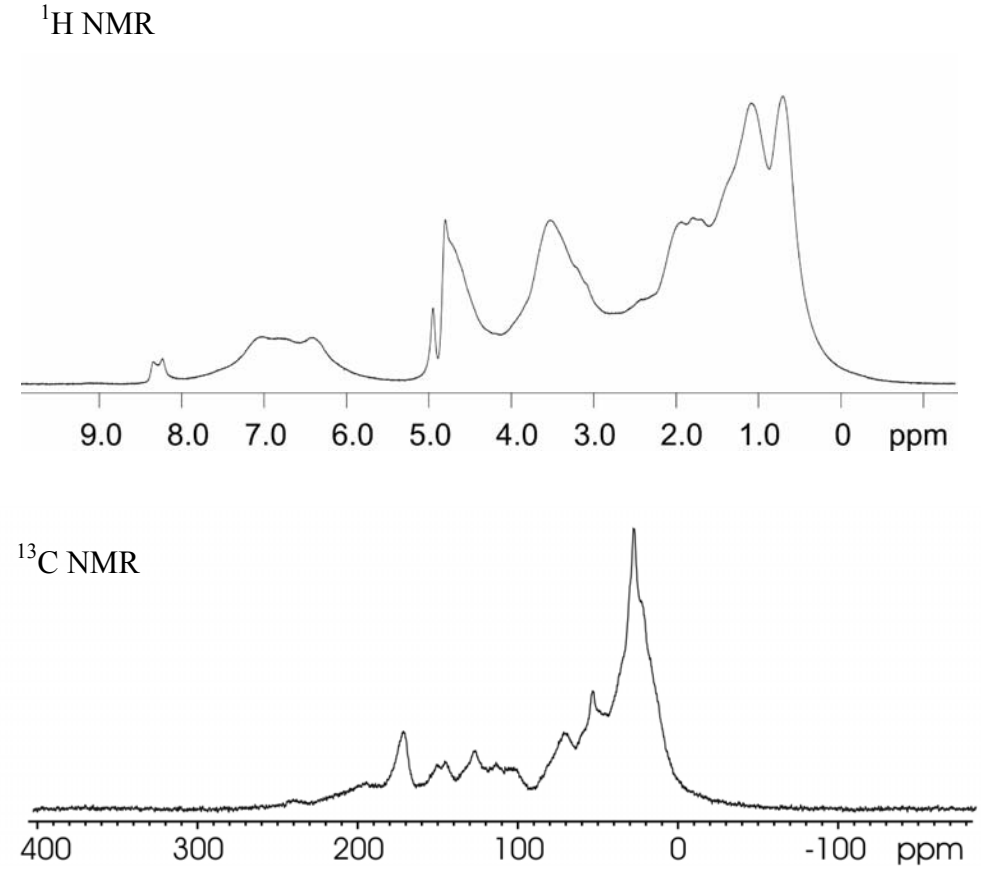

Fig. 3. Proton and carbon NMR spectra of cHAL2.

The IR spectra of the two humic acid-like compounds were also consistent with the presence of several functional groups and C bonds. IR peak absorbances were found at 1718 cm^{-1} for free carboxylic acid groups, at 1518 cm^{-1} for amide groups, at 1458 cm^{-1} for aromatic rings, at 1278 cm^{-1} for C-O bonds in phenol, phenyl ether, and COOH groups, in the 2000-3700 cm^{-1} range for O-H and/or N-H groups in COOH, phenol, amide groups, and carbohydrates, and at 2928 and 2855 cm^{-1} for protonated aliphatic C chains (Quagliotto 2006). In agreement with the NMR spectra the IR spectrum of cHAL2, compared to that of cHAL, showed higher intensity of the bands assigned to protonated aliphatic C chains and OH groups relatively to the bands assigned to C-O bonds in phenol, phenyl ether, and COOH groups. These features are likely to be memory of the main molecular constituents of the investigated green wastes such as polysaccharides, protein, lipids, and lignin. Particularly the higher content of O-alkyl and di-Oalkyl C in cHAL2, which is supported by the relatively higher intensities of both the ^{13}C NMR signals at 53-110 ppm (Table 2) and of the ^{1}H NMR signals at 2.5-4.2 ppm (Table 3), is equivalent to the presence of 1 carbohydrate hexose fragment per two aromatic rings.

Table 2. Assignments by Chemical Shift (δ, ppm)ranges and Relative Area of ^{13}C CPMAS NMR Bands, and C Distribution per Molecular Fragment Containing Two Aromatic Rings.

	Assignment	1 Aliphatic C bonded to other aliphatic chain or to H		2 Total alipha-tic C	3 O-CH_3 or N-alkyl C	4 O-alkyl C	5 di-O-alkyl C	6 Aro-matic C	7 Phenol or phenyl ether C	8 Carbox-yl C	9 Keto C	10 Other C
		Short chain	Long chain									
	band δrange (ppm)	0-32	32-53	0-53	53-63	63-95	95-110	110-140	140-160	160-185	185-215	215-250
cHAL	band relative area (%)	32.3	12.9	45.2	8.4	9.2	3.5	14.8	6.8	11.5	0.6	-
	C distribution for two aromatic rings	17.9	7.2	25.1	4.7	5.1	1.9	8.2	3.8	6.4	0.33	-
cHAL2	band relative area (%)	36.0	13.6	49.5	6.5	11.5	3.6	9.1	5.1	7.4	4.6	2.6
	C distribution for two aromatic rings	30.4	9.5	39.9	5.5	9.7	3.0	7.7	4.3	6.2	3.9	2.2

Table 3. Assignments by Chemical Shift (δ, ppm) ranges and Relative Area of ^{1}H NMR Bands

	H in aliphatic C for hydrocarbon chains substituted at β or farther C, or in CH2 and CH3 bonded to aromatic C, or to carboxylic or amide groups		H in methine group bonded to aromatic C, or in aliphatic C bonded to O or to N	aromatic and olefinic H
band δ range (ppm)	0-1.2	1.2-2.9	2.9-4.3	5.9-8.1
cHAL2	23.6	39.0	26.5	10.9
cHAL	47.2	28.1	15.1	9.6

This molecular fragment is unlike to represent evidence of poly- or oligo-saccharide molecules simply mixed with the humic acid-like matter, since this material has been isolated by precipitation at pH < 1.5 (Montoneri 2003a). We rather favour the hypothesis that the above fragment was bonded covalently to the alkyl-phenoxy lignin-like part of the humic acid-like molecule. The higher content of fragments with carbohydrate structure in cHAL2 than in cHAL seems consistent with the different origin of these materials. Indeed, cHAL is a humic acid-like compound isolated from a refuse subjected to aerobic biodegradation for 15-d. Therefore, considering the longer biodegradation of cHAL relatively to cHAL2, a higher content of molecular fragments with carbohydrate structure is to be expected in the latter for thermodynamic and kinetic reasons (Montoneri 2003b). Also, it may be observed that the ^{1}H NMR spectra (Table 3) indicate a relatively higher content of aromatic H in cHAL2 than in cHAL. This fact, coupled with the relatively lower content of aromatic C indicated by the ^{13}C data (Table 2), suggests that the aromatic rings in cHAL2 are both fewer and less substituted. In turn, the lower substitution degree of the aromatic rings in cHAL2 seems consistent with the lower content of phenoxy groups reported in Table 1.

As most of the potential technological appeal of compost isolated humic acid-like substances have been inferred by us (Quagliotto 2006) to lie on their surface activity properties in solution, surface tension measurements constitute a basilar characterization for these compounds. Surfactants properties for cHAL2 were expected based on its structural analogies with cHAL and naturally occurring humic acids, i.e., presence of hydrophobic C chains and of polar groups. In principle, surfactants should give a surface tension (γ) versus concentration (C) plot where two clear linear regimes, premicellar and postmicellar, are evidenced. This is mostly found for simple surfactant molecules with one polar head. Oligomeric surfactants, such as the gemini surfactants (Quagliotto 2006) show a gradual transition between the two regimes, whose extension may be very large. These surfactants are made of molecules in which two or more polar groups are connected by lipophilic chains of variable length. Their oligomeric or polymeric nature is a key point in determining their capacity to micellize. The same could be expected for humic-like substance. When these materials are in solution as single molecules, these lie at the air-water interface to expose as the lowest possible hydrophobic surface to water. At higher concentration, when the air-water interface is saturated, the excess surfactant molecules aggregate forming micelles in the bulk water phase. In this form several molecules are held together by intermolecular forces to yield spherical or quasi-spherical clusters where hydrophobic surfaces stay in the inner micellar core and polar heads are directed toward the water phase. In a typical case, the premicellar and the postmicellar regimes are defined by two linear γ–C with different slopes. The intersection of the two

lines gives the cmc. For cHAL2, the results of our surface tension measurements against concentration are shown in Fig. 4. From the γ–C plot the slope change can easily be identified and the cHAL2 critical micellar concentration (cmc) and the surface tension at the cmc (γcmc) may be calculated 0.97 g L^{-1} and 37.8 mN/m. These values are higher than those reported for cHAL, i.e., cmc = 0.40 g L^{-1} and γcmc = 36.1 mN/m (Quagliotto 2006). Although the higher content of aliphatic C of cHAL2 usually would lead one to expect a lower cmc value than that of cHAL, the higher content of polar functional groups contributed by the O-alkyl and di-O-alkyl C in the former may introduce a higher degree of hydrophilicity that hinders micelles formation (Sulthana 2000). A similar effect has been reported for humic acids isolated from peat and soil upon increasing the relative content of carboxylic groups (Quagliotto 2006).

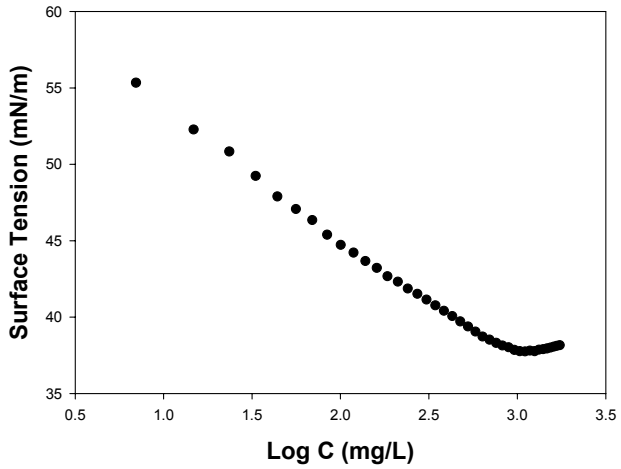

Fig. 4. Surface tension versus concentration (Log C) for cHAL2 water solution at pH 7

One structural feature of humic acid-like material which is currently a matter of dispute is their molecular weight (Sutton 2005). Measurements based on size exclusion chromatography (SEC) indicate values of the order of 10^4-10^5 D, whereas measurements performed by electrospray ionization (ESI) indicate values of the order of 10^3 Da. The ESI results, coupled with the fact that by gel permeation chromatography and high-pressure size-exclusion chromatography some workers have found that the apparent size of humic fragments changes drastically with addition of simple organic acids, has originated the belief that humic acid-like substances are aggregates of small molecules linked by hydrogen bonds and hydrophobic interactions, and not polymeric compounds containing covalent bonds only. The dispute over the molecular weight of humic acid-like substances is not only academic, but has relevance in relation to the performance of these materials as surfactants. With specific reference to our cHAL2 material, assessing the size of the molecules which give rise to the curve in Fig. 4 would make it possible to establish structure-properties relationships and then to use these in order to exploit the full potential of the material for specific technological applications. Thus, in this paper, we have address the molecular weight issue based on considerations and on experimental results which are described hereinafter.

In principle humic acid-like substances may yield two types of conformation in solution, which may be responsible for important interaction with other organic and inorganic species. These may be classified as micelles and pseudo-micelles (von

Wandruszka 2000). Whereas the former are aggregates of relatively small molecules held together by intermolecular forces, the latter may be visualized as macromolecules which, by virtue of the flexibility of the C chain, may fold and coil in a manner that directs hydrophilic (e.g. carboxy and hydroxy) groups outward and keeps more hydrophobic (e.g. hydrocarbon) moieties isolated in the center. This process produces an entity that is operationally similar to a conventional micelle, albeit more structurally constrained. Like a micelle, it has a hydrophobic interior and a more hydrophilic surface, giving it distinct solubilizing powers for nonpolar solutes. For our cHAL2 materials, we have carried out measurements of the molecular size and mass by three different techniques: i.e., ESI, SEC-MALS and DLS.

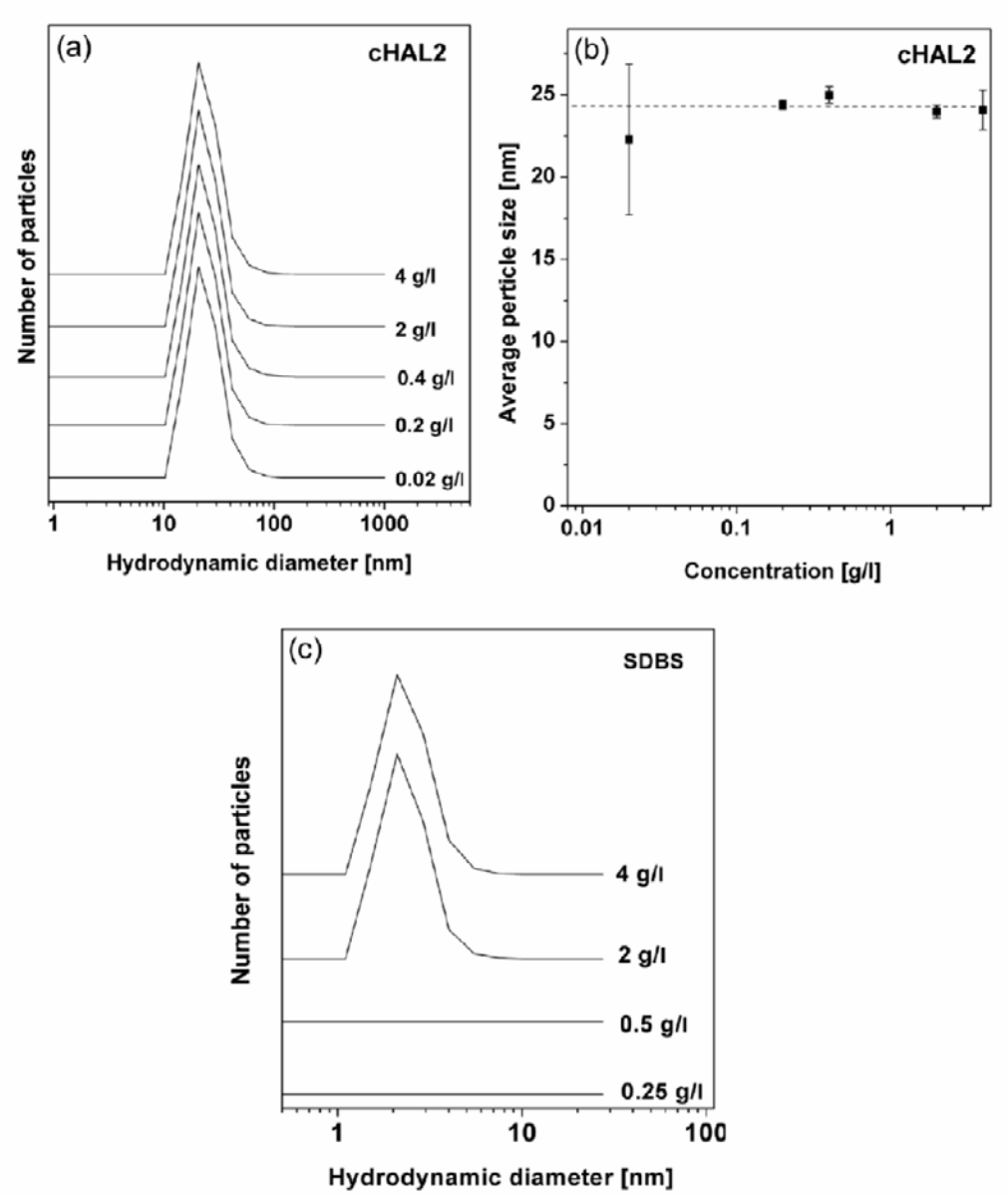

Fig. 5. Comparison between the particle size at different concentrations of cHAL2 (a and b) and the commercial additive SDBS (c). The particle size distribution of the two surfactants was measured at concentrations above and below the respective cmc values.

Dynamic light scattering (DLS) theory is a well established technique for measuring particle size over the 10^{-10}-10^{-6} m range (Microtrac, Inc. 2007). DLS measures the velocity at which particles within a solvent diffuse due to Brownian motion. This is done by monitoring the fluctuation in intensity of the scattered light over the time. Indeed the scattered intensity due to the phase addition of the moving particles is constantly evolving, depending on the particle size. The Brownian diffusion velocity is inversely proportional to the particles size, expressed as hydrodynamic diameter (D_h). As this technique allows the determination of particle size distributions in solution at variable concentration, and therefore allows the calculation of the hydrodynamic diameter of the molecules or aggregates in solution, we performed DLS measurements at variable cHAL2 concentration (0.02-0.2 g L^{-1}). Based on our surface tension data (reported above) indicating formation of micelles for cHAL2 at 0.97 g L^{-1}, we expected by carrying DLS measurements below and above this concentration value to observe a change of D_h with cHAL2 concentration; i.e., a D_h increase above the 0.97 g L^{-1} value due to the formation of molecular aggregates. Contrary to this expectation the plots in Fig. 5 do not show any significant change of D_h with concentration. The DLS measurements were repeated three times for each sample, and an average D_h value was calculated for every concentration. In Fig. 5b the average size, as calculated from three measurements, is reported as function of the concentration. The vertical bars indicate the standard deviation for every set of measurements. The data suggest that cHAL2 consists of particles with sizes included between 10 and 100 nm, and that this particle size distribution does not change upon changing the sample concentration. An average D_h of 24.4 nm was extrapolated from all the data here presented.

The same particle size was found by DLS measurements of a reference humic acid (HA) sample isolated from Suwannee River and supplied by the International Humic Substance Society (IHSS, St. Paul, USA) which was analyzed in solution at pH 7 and 0.04 g/L concentration (Baalousha 2006). The sizes measured for cHAL2 and the IHSS HA do not imply the absence of smaller particles. In fact, scattering intensity is inversely proportional to the sixth power of the radius for particles smaller than the wavelength of the laser; thus, larger particles scatter light more effectively than smaller ones. Therefore, large particles mask the presence of smaller ones in the sample. By comparison, we performed the same measurement on sodium dodecylbenzenesulfonate (SDBS). This well known synthetic commercial surfactant is reported to form micelles at 0.7-1.4 g L^{-1} concentration in water and at pH 7 (Savarino 2007). With this molecule, our DLS measurements (Fig. 5c) showed signals at 2-4 g L^{-1} concentration, whereas below the surfactant cmc value (0.25-0.50 g L^{-1}) the concentration the scattered intensity was extremely low and only the noise due to impurities bigger than 30 nm in the solution was detectable. In may be observed that the range of particle size for the SDBS small molecule is one order of magnitude lower than that observed for cHAL2. Also, contrary to the cHAL2 case, the data for SDBS indicate an increase of the particle size above the surfactant cmc value. The SDBS data therefore prove that DLS may show aggregate formation for small molecules, in the absence of large masking particles. By comparison, the lack of change of D_h with cHAL2 concentration, and therefore the absence of correlation between DLS and surface tension data, suggest that the large particles observed by DLS are not responsible for the surface tension dependence on concentration shown in Fig. 4, since their size seems unchanged over a very wide concentration range. Although the data do not make it possible to assess whether the large particles are aggregates or macromolecules, other small molecules must be present together with the larger particles. The small molecules would aggregate upon raising the cHAL2 concen-

tration and be responsible of the change of surface tension observed in Fig. 4. Evidence for the presence of both small molecules and large molecules was sought by the other two techniques, SEC-MALS and ESI.

In the SEC-MALS measurements the optimisation of the solubilization procedure and of the SEC experimental conditions for humic acid-like substances is not trivial. As reported in literature (Quagliotto 2006) and shown hereinafter, humic acid-like substances in aqueous solution are strongly aggregated and may yield micelles of various sizes. Furthermore, the aggregation extent may be significantly affected (Terashima 2004) by pH, ionic strength, and type of counterion of the used solvent. In addition to this, the SEC fractionation for these substances is a problem because column non-steric separation could occur. Often upon using non-optimized SEC conditions, multimodal and/or asymmetrical chromatograms with very long tails are obtained. With cHAL2 in the water- methanol solvent (see experimental), we have obtained a quasi-symmetrical chromatogram without a long tail, as opposed to asymmetrical long tail chromatograms obtained in the pure aqueous solvent. This fact suggested minimization of any presumable molecular aggregation due to the presence of methanol in the sample and elution solvent.

Figure 6 reports the experimental differential refractometer index (DRI) and light scattering (LS) signals, and the calculated molar mass (M) as a function of the elution volume (V). The M=*f*(V) experimental function is the classical SEC calibration curve obtained directly from the on-line MALS detector. Using the M=*f*(V) experimental function and the DRI curve, the molar mass distribution (MMD) for the cHAL2 sample reported in Fig. 7 was obtained. A summary of the molecular characterization of this sample is reported in Table 4. Basically, the cHAL2 sample shows an apparent molar mass centred around 150 kg/mol with a polydispersity of about 1.5-2.

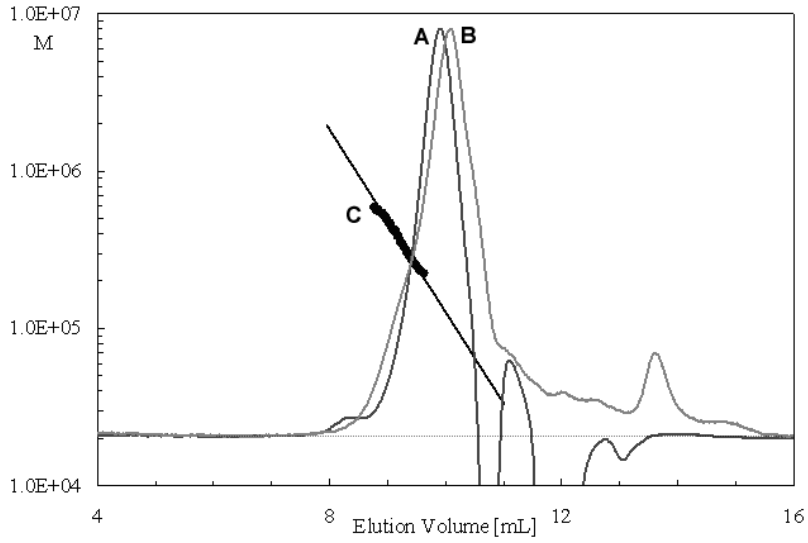

Fig. 6. Superimposition of concentration by DRI (curve A)and MALS with photodiode located at 90° (curve B)signals together with the calculated molar mass (M) as a function (line C) of the elution volume (V) for the cHAL2 sample.

Table 4. SEC-MALS Molecular Characterization[a] of cHAL2.

M_p	M_n	M_w	M_z	M_w/M_n	M_z/M_w
g/mol	g/mol	g/mol	g/mol		
143,400	149,340	217,630	432,340	1.5	2.0

[a]Molar mass of the chromatographic peak (M_p), number- (M_n), weight- (M_w) and z- (M_z) molar mass averages, and polydispersity indexes M_w/M_n and M_z/M_w.

The on-line MALS detector is also able to measure the molar mass (M) of the eluting fractions together with the dimension of the macromolecules, which is generally known as radius of gyration (Rg). This latter parameter is measured from the angular variation of the scattering intensity, when this is approximately higher than 8-10 nm. The Rg = f(M) experimental function, (i.e., the conformation plot) of the cHAL2 sample is shown in Fig. 7. It is evident that the dimensional Rg parameter for the cHAL2 sample approximately ranges from 10 nm to 20 nm. Furthermore, from the estimated slope of the conformation plot (approximately 0.4) a compact quasi-spherical conformation of the cHAL2 aggregate or molecule could be inferred. The above 10-20 nm Rg value measured by SEC-MALS is consistent with the results obtained by DLS. By comparison, the molecular radius of naturally occurring humic acids has been reported to increase from 9.8 to 17.8 Å as the molecular weight increases from 5000 to 30000 (Tan 2003). Similarly to the DLS results, the SEC-MALS do not provide evidence of the presence of small molecules.

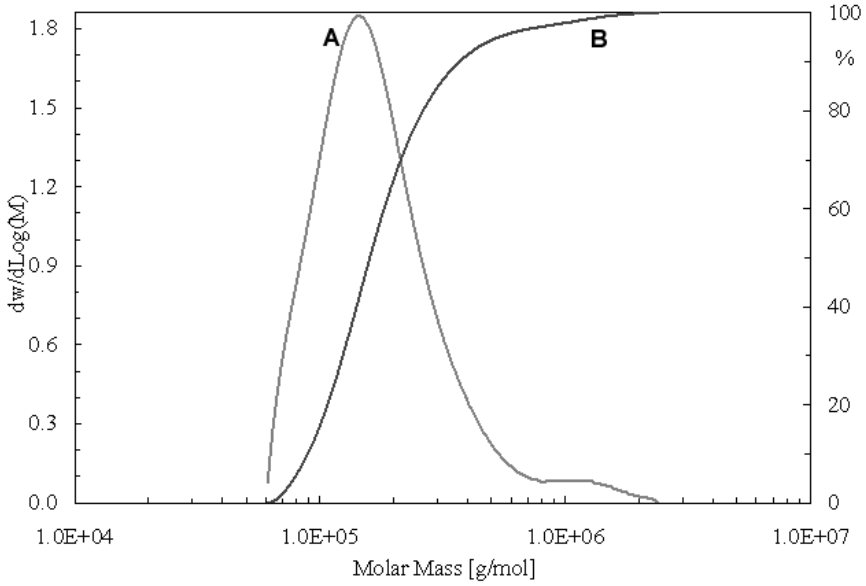

Fig. 7. Differential [dw/dLog(M) for curve A] and cumulative (% for curve B) molar mass distribution (MMD) from SEC-MALS measurements for the cHAL2 sample.

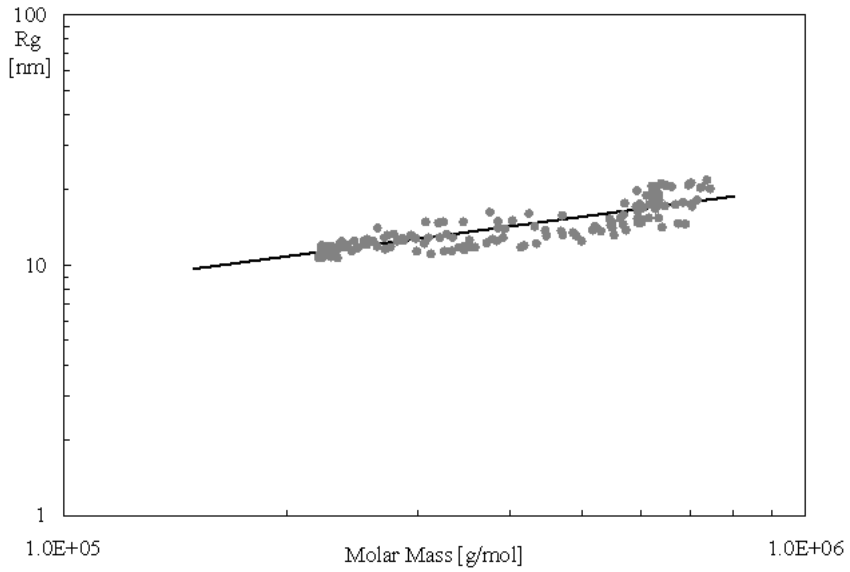

Fig. 8. Conformation plot from SEC-MALS of the cHAL2 sample; radius of gyration (Rg) as a function of molar mass.

Soft desorption ionization techniques, such as electrospray ionization (ESI), volatilize large ions for identification via mass spectrometry (MS), providing positive or negative ion mass/charge distributions that may represent the mass distribution of molecules within humic fractions (Sutton 2005). By this technique compounds may be analyzed from aqueous or aqueous/organic solutions at variable concentrations, similarly to the case of the above DSL measurements. As solvent evaporation occurs, the droplet shrinks until it reaches the point that the surface tension can no longer sustain the charge (the Rayleigh limit). At this point a "Coulombic explosion" occurs and the droplet is ripped apart. This event produces smaller droplets that can repeat the process as well as naked singly or multiply charged analyte molecules. High resolution mass spectrometry makes it possible to assign the charge value to an ESI signal originated by an ionized molecule through the examination of the signal isotopic peaks intensity.

Our ESI measurements were performed on cHAL2 and SDBS solutions at the same pH and sample concentrations as for the DLS measurements. The results of the ESI measurements for cHAL2 showed that below the surfactant sample cmc value the signals intensity was too low to allow any useful analysis of the recorded mass spectra. Above the cmc value, several significant signals were observed over the investigated 200-1500 m/z range (Fig.8). For the main signals falling in the 400-450 m/z range, z was proven equal to 1 by the distinctive isotopic pattern for singly charged ions which was observed in the spectra acquired at 60000 resolving power. Also, above the cHAL2 cmc value, the relative intensity of these signals was shown to increase linearly with the sample concentration. The same could not be assessed for the signals at m/z > 500. Although several signals at these m/z values are present in Fig. 9, their relative intensity did not change significantly with the sample concentration. These signals therefore were assigned to the measurements background noise and were not further analyzed for our scope. By comparison for the SDBS solutions in the 0.02 and 2 g L^{-1} concentration range, which included the 0.7-1.4 g L^{-1} values reported for the cmc of this compound (Savarino 2007), the signal of the $C_{12}H_{25}(C_6H_4)SO_3^-$ anion at 325 m/z was well observed, together with

other two signals at 311 and 339 m/z which were likely to arise from $C_{11}H_{23}(C_6H_4)SO_3^-$ and $C_{13}H_{27}(C_6H_4)SO_3^-$ impurities. For this compound, the intensity of these signals increased linearly with concentration, but the same did not occur for the higher m/z signals, which were therefore assigned to the background noise. The results obtained for SDBS demonstrate that ESI is not able to assess the presence of molecular aggregates, as the weak interactions holding these species are broken during spray ionization. However, for the present work, the ESI results are highly important, inasmuch as they prove the presence of small molecules with molecular weights around 450 in the cHAL2 humic-like material, nearly half the weight of the fragment represented in Fig. 2. The enlarged spectra in the lower m/z region revealed repetitious peaks at discrete 14 Da. These suggest the presence of molecules with methylene chain of different lengths and are consistent with the above discussed NMR and IR spectroscopy findings. The ESI results also do not exclude the presence of larger molecules, as these might not volatilize under the analytical experimental conditions. Although the results obtained by the above three techniques together suggest the presence of small molecules together with large macromolecules, the real molecular mass distribution in the cHAL2 sample cannot be assessed.

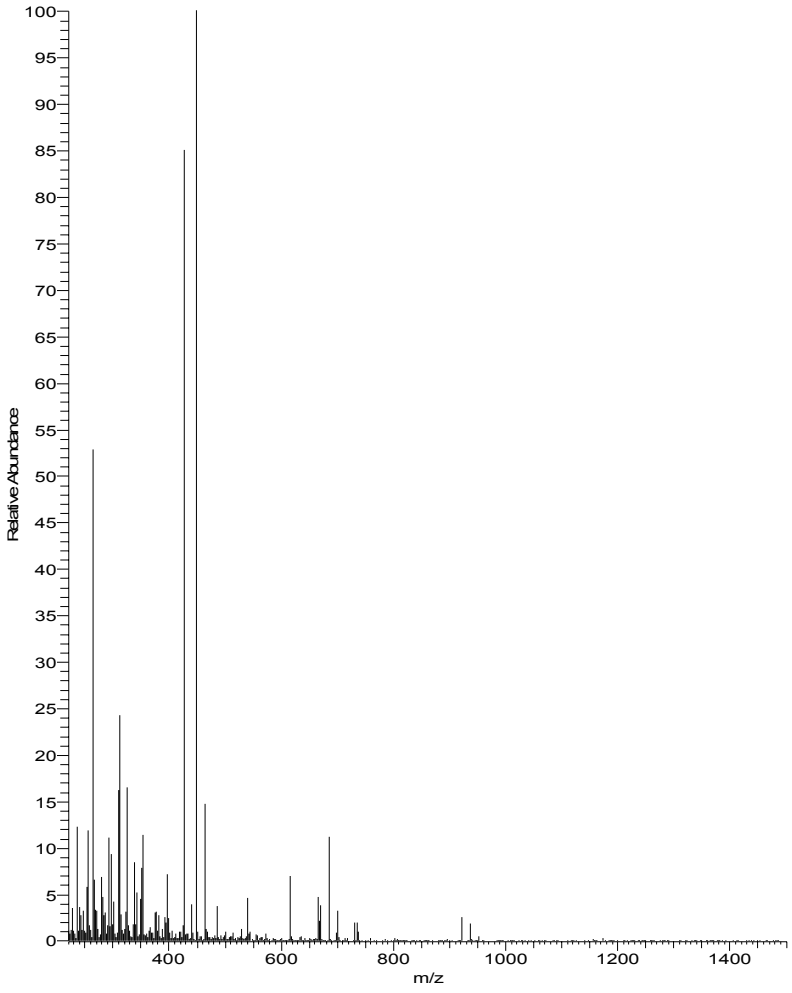

Fig. 9. Negative ion mode ESI spectrum acquired starting from 2.0g L^{-1} cHAL2 solution at pH7.

CONCLUSIONS

We have shown that two humic acid-like substances isolated from two different urban waste sources have different chemical structural features that significantly affect their surfactants properties. The results point out that biomass wastes may be an interesting source of biosurfactants with diversified properties that depend on the nature of waste and of its treatment process. Our structural investigation on cHAL2 suggests that, similarly to naturally occurring humic acids (HAs), it is likely to be a mixture of small molecules with molecular weight of the order of few thousands Da or less, and macromolecules with molecular weights of several hundred thousands. Whereas the size of the latter is not affected by their concentration in water, the small molecules probably can aggregate and be responsible for the surface tension versus concentration behaviour shown in Fig. 4. As to the potential performance of this humic acid-like substance in chemical technology, these materials could perform as classic surfactants due to their content of small molecules and capacity to yield micelles, and as dispersants due to their content of macromolecules (Showell 2006). In the next part of this work (Montoneri 2007, "Part 2") we will report the performance of cHAL2 as an auxiliary in a few important chemical technological applications and discuss the significance of the above structural features on performance rate.

ACKNOWLEDGMENTS

This work was carried out with Regione Piemonte Cipe 2004 funds for Cod. C 13 sustainable development program. This contribution was an original presentation at the *ITALIC 4 Science & Technology of Biomass: Advances and Challenges* Conference that was held in Rome, Italy (May 8-10, 2007) and sponsored by Tor Vergata University. The authors gratefully acknowledge the efforts of the Conference Organizers, Prof. Claudia Crestini (Tor Vergata University, Rome, Italy), Chair, and Prof. Marco Orlandi (Biococca University, Milan, Italy), Co-Chair. Prof. Crestini also is Editor for the conference collection issue to be published in *BioResources.*

REFERENCES CITED

Baalousha, M., Motelica-Heino, M. and Le Coustumer, P. (2006). "Conformation and size of humic substances: Effects of major cation concentration and type, pH, salinity, and residence time," *Colloids and Surfaces A: Physicochem. Eng. Aspects* 272, 48–55.

Brunelot, G., Adrian, P., Roulller, J., Guillet, B., and Andreoux, F. (1989). "Determination of dissociable acid groups of organic compounds extracted from soils, using automated potentiometric titration," *Chemosphere* 19, 1413-1419.

Genevini, P. L., Adani, F., Veeken, A., Nierop, G. J., Scaglia, B., and Dijkema, C. (2002). "Qualitative modifications of humic acid-like and core-humic acid-like during high-rate composting of pig faeces amended with wheat straw," *Soil Sci. Plant Nutr.* 48, 143–150.

Gran, G. (1952). "Determination of the equivalence point in potentionmetric titrations. Part II," *Analyst* 77, 661-671.

Guetzloff, T. F., and Rice, J. A. (1994). "Does humic acid form a micelle?" *Sci. Total Environ*. 152, 31-35.

Kawahigashi, M., Sumida, H., and Yamamoto, K. (2005). "Size and shape of soil humic acids estimated by viscosity and molecular weight," *J. Coll. Interf. Sci*. 284, 463–469.

Kraft, E., Bidlingmaier, W., De Bertoldi, M., Diaz, L. F., and Barth, J. (Eds.) (2006). *Proceedings of the International Conference Orbit 2006 Biological Waste Management from Local to Global*. Weimar: verlag ORBIT e.V.; ISBN 3-935974-09-4.

Mendichi, R., and Giacometti Schieroni, A. (2001). "Use of a multi-detector size exclusion chromatography system for the characterization of complex polymers," *Current Trends in Polymer Science,* Pandalai S.G. Ed., Trans-World Research Network: Trivandrum India, Vol. 6, pp. 17-32.

Montoneri, E., Savarino, P., Adani, F., Genevini, P. L., Ricca, G., Zanetti, F., and Paletti S. (2003a). "Polyalkylphenyl-sulphonic acid with acid groups of variable strength from compost," *Waste Management* 23(6), 523-535.

Montoneri, E. (2003b). "Organic matter of compost" *Workshop Proceedings On the Role of Organic Matter in a Sustainable Agriculture,* Villa Marigola, Lerici, June 5-6, pages 84-88.

Montoneri, E., Savarino, P., Bottigliengo, S., Musso, G., Bianco Prevot, A., Fabbri, D., and Pramauro, E. (2007). "Humic acid-like matter isolated from green urban wastes. Part II: Performance in chemical and environmental technologies," *Bioresources*, submitted for publication.

Microtrac, Inc (2007). "Dynamic light scattering," available at http://www.microtrac.com/dynamicscattering.cfm [accessed August 2007].

Newman, D. (2006). "Compostaggio in Italia, riflessioni sulle opportunità e prospettive future*,"* paper presented at the meeting on *Recupero dei rifiuti industriali organici: conversione dei rifiuti in risorsa*, held at the University of Torino on December 13.

Ozores-Hampton, M., and Obreza, T. (2007). "Beneficial uses of compost in Florida vegetables crops," *Compost facilities in Florida.pdf,* available at www.imok.ufl.edu/compost/pdf/Compost_Utilization.pdf [accessed April 13, 2007].

Provencher, S. W. (1976). "A fourier method for the analysis of exponential decay curves," *Biophys. J.* 16, 27–41.

Quagliotto, P. L., Montoneri, E., Tambone, F., Adani, F., Gobetto, R., and Viscardi, G. (2006). "Chemicals from wastes: Compost-derived humic acid–like matter as surfactant," *Environ. Sci. Technol*. 40, 1686-1692.

Rosen, M. J. (Ed.) (1989). *Surfactants and Interfacial Phenomena*, 2nd edition, Wiley, New York. (forse eliminare)

Savarino, P., Montoneri, E., Biasizzo, M., Quagliotto, P. L., Viscardi, G., and Boffa, V. (2007). "Upgrading biomass wastes in chemical technology. Humic acid-like matter isolated from compost as chemical auxiliary for textile dyeing," *J. Chem. Tech. Biotech.* in the press.

Showell, M. S. (Ed.) (2006). *Handbook of Detergents. Part D: Formulation*, Taylor & Francis, Boca Raton, Fl (USA).

Stoffella, P. J., Li, Y., Roe, N. E., Ozores-Hampton, M., and Graetz, D. A. (1997). "Utilization of composted organic wastes in vegetable production systems," Food & Fertilizer Technology Center Bulletin 1997-12-01, available at http://www.agnet.org/library/abstract/tb147.html [accessed April 13, 2007].

Sulthana, S. B., Bath, S. G. T., and Rakshit, A. K (2000). "Solution properties of sodium

dodecylbenzenesulfonate (SDBS): Effects of additives," *Bull. Chem. Soc. Jpn*. 73, 281-287.

Sutton, R., and Sposito, G. (2005). "Molecular structure in soil humic substances: The new view," *Environ. Sci. Technol*. 39, 9009-9015.

Tan, K. H., (ed.) (2003). *Humic Matter in Soil and Environment. Principles and Controversies*; Chapter 6; Marcel Dekker, Inc., New York.

Terashima, M., Fukushima, M., and Tanaka, S. (2004). "Influence of pH on the surface activity of humic acid: Micelle-like aggregate formation and interfacial adsorption," *Colloids and Surfaces A: Physicochem. Eng. Aspects* 247, 77-83.

von Wandruszka, R. (2000). "Humic acids: Their detergent qualities and potential uses in pollution remediation," *Geochem. Trans*. 1(2), 10-15.

Article submission received: Sept. 21, 2007; Peer-review completed, Dec. 15, 2007;
Revised version received and accepted: Dec. 17, 2007; Published Dec. 20, 2007.